NASA TECHNICAL NOTE

NASA TN D-3630

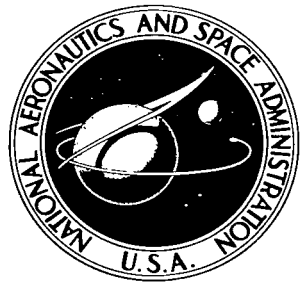

NASA TN D-3630

DAMAGE TO FIELD-EFFECT TRANSISTORS UNDER 22 AND 128 MeV PROTON BOMBARDMENTS

by Floyd R. Bryant and Carl L. Fales

Langley Research Center
Langley Station, Hampton, Va.

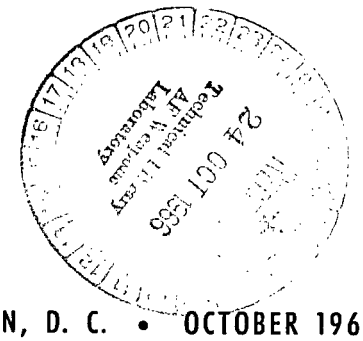

NATIONAL AERONAUTICS AND SPACE ADMINISTRATION • WASHINGTON, D. C. • OCTOBER 1966

DAMAGE TO FIELD-EFFECT TRANSISTORS UNDER 22 AND 128 MeV PROTON BOMBARDMENTS

By Floyd R. Bryant and Carl L. Fales

Langley Research Center
Langley Station, Hampton, Va.

NATIONAL AERONAUTICS AND SPACE ADMINISTRATION

For sale by the Clearinghouse for Federal Scientific and Technical Information
Springfield, Virginia 22151 – Price $2.00

DAMAGE TO FIELD-EFFECT TRANSISTORS UNDER 22 AND 128 MeV PROTON BOMBARDMENTS

By Floyd R. Bryant and Carl L. Fales
Langley Research Center

SUMMARY

Silicon n- and p-channel planar diffused junction, silicon n-channel epitaxially grown junction, and germanium n-channel alloy junction field-effect transistors were irradiated with 22 and 128 MeV protons at the Oak Ridge National Laboratory 22 MeV cyclotron (nine types of devices) and at the Harvard University 168 MeV synchrocyclotron (two types).

Transistor curve tracer photographs of the drain characteristic curves were obtained at various integrated proton flux levels and several electrical parameters were determined at the NASA Langley Research Center prior and subsequent to irradiation. Drain current and the approximate transconductance in the pinch-off operation region of the field-effect transistor were computed from the characteristic curves.

In particular, the zero-gate-voltage drain current and transconductance are examined in some detail. Simple theory from a model based on initial carrier removal rate indicates linear and quadratic dependence of zero-gate transconductance and drain current, respectively, on integrated proton flux. For illustrative purposes, three transistor types, all bombarded with 22 MeV protons, were examined to study this effect. Two types possess zero-gate-transconductance variations in reasonable accord with the anticipated first-degree dependence. In contrast, the curve of the zero-gate drain current as a function of flux data of the third type adapts nicely to a straight-line fit. Also, the quadratic dependence of the zero-gate-voltage drain current fails, but a power-law relation with proton flux holds and the exponents range from 1 to 1.6. Plots of normalized zero-gate drain current and transconductance as functions of integrated proton flux are presented. Significant spread exists among the responses of the transistors of a particular type to the damaging radiation. No attempt was made to match transistor parameters prior to the experiments. Several miscellaneous results of the irradiation tests are discussed and some accountability for the deviations from theory is presented.

Despite the partial agreement with a theoretical model, accurate radiation damage prediction techniques for the field-effect transistor are not readily obtainable because of the initial spread in irradiation responses of the transistors. On a more favorable note, it was found that many field-effect transistors possess a radiation resistance to 22 and 128 MeV protons at least comparable to most narrow-base minority carrier devices.

INTRODUCTION

Unlike the conventional transistor, the action of which depends upon the transport of minority carriers through the base region, the field-effect transistor (FET) is a majority carrier semiconductor device. From the standpoint of radiation damage, it is expected that the field-effect transistor will frequenctly possess a greater resistance to radiation than the conventional transistor. This conclusion is drawn from experimental data (e.g., refs. 1 and 2) on semiconductors having resistivities typical of field-effect transistors. The references indicate that minority carrier lifetime, on which the current gain of the standard transistor relies most heavily, decreases more rapidly under displacement-producing radiation than does carrier concentration and mobility, upon which the drain current and transconductance of the field-effect transistor depend.

Despite improved resistance to radiation, the electrical characteristics of the field-effect transistor can undergo critical degradation in intense radiation fields. Specifically, the interest here is in the energetic protons existing in a space environment.

Due to low noise characteristics (ref. 3), high-input impedance, and reported relatively high radiation resistance to electrons and neutrons (refs. 4 and 5), field-effect transistors are generating new interest among circuit designers in space programs. Typical applications are high-input impedance transducer amplifiers and preamplifiers, low-noise receivers, differential amplifiers, and switching circuits.

Because of the potential applications of field-effect transistors in space systems and the fact that proton irradiation data at energies typical of a space environment are not extensive, an experimental evaluation of field-effect transistors in a proton environment was initiated.

Nine types of field-effect transistors were bombarded with 22 MeV protons at the Oak Ridge National Laboratory 22 MeV cyclotron and two types were bombarded with 128 MeV protons at the Harvard University 168 MeV synchrocyclotron. Parameters measured before and after irradiations were: zero-gate-voltage drain current, gate-source cut-off current, drain-gate leakage current, source-gate leakage current, drain-gate breakdown voltage, transconductance, gate pinch-off voltage (at designated values of drain current and voltage), and for several transistors, small-signal common source input admittance.

The common-source drain characteristics were recorded at various levels of integrated proton flux.

SYMBOLS

a	one-half channel thickness
BV_{DGO}	drain-gate breakdown voltage
C_g	capacitance
C_i	arbitrary constant, $i = 1, 2, 3, \ldots$
E	energy
f	frequency
g_d	small-signal drain conductance, $\left(\frac{\partial I_D}{\partial V_D}\right)_{V_G=\text{Constant}}$
g_m	transconductance, $\left(\frac{\partial I_D}{\partial V_G}\right)_{V_D=\text{Constant}}$
$g_{m,0}$	zero-gate-voltage transconductance
I_D	drain current
I_{DG}	drain-gate current
I_{DGO}	drain-gate leakage current
I_{DS}	drain-source current
I_{DSS}	zero-gate-voltage drain current
I_{SGO}	source-gate leakage current
I_{GSS}	gate-source cut-off current

$$J(V) = 2\sigma a V\left[1 - \frac{2}{3}\left(\frac{2KV}{\rho a^2}\right)^{1/2}\right]$$

K	dielectric constant
l	length of channel
n	mobile electron or carrier concentration
Q_c	zero-gate-voltage channel mobile charge
q	electronic charge
R_{in}	input resistance
R_s	degenerative channel resistance
V	voltage
V_D	drain voltage
V_G	gate voltage
V_P	gate pinch-off voltage
V_S	source voltage
V_{DS}	drain-source voltage
V_{GS}	gate-source voltage
V_{SG}	source-gate voltage
W_o	saturation voltage
$\bar{x}$	coordinate position vector
y_{is}	small-signal common source input admittance
z	channel width

$$\gamma = \frac{1}{n_o}\left(\frac{dn}{d\phi}\right)_o$$

μ majority carrier mobility

ρ donor charge density, mobile carrier charge density of extrinsic n-type semiconductor

σ bulk conductivity $= \rho\mu$ for extrinsic n-type semiconductor

ϕ integrated flux

ϕ_t total integrated flux

$\frac{dn}{d\phi}$ carrier removal rate

Subscripts:

o initial condition (before irradiation)

O open circuit

S short circuit

Notations:

Ge germanium

Si silicon

APPARATUS AND PROCEDURE

Silicon n- and p-channel planar diffused junction, silicon n-channel epitaxially grown junction, and germanium n-channel alloyed junction field-effect transistors were irradiated with 22 and 128 MeV protons at the Oak Ridge National Laboratory 22 MeV cyclotron and at the Harvard University 168 MeV synchrocyclotron, respectively. A general description of each transistor bombarded in the experiments is shown in the following table:

Transistor	Description	Structure
Type A	n-channel Si	Epitaxial
Type B	p-channel Si	Diffused
Type C	p-channel Si	Planar diffused
Type D	n-channel Si	Epitaxial
Type E	n-channel Si	Planar
Type F	n-channel Si	Epitaxial
Type G	n-channel Si	Epitaxial
Type H	p-channel Si	Planar
Type J	n-channel Ge	Alloy junction
Type K	n-channel Si	Epitaxial

Experimental arrangements similar to that shown in figure 1 were employed at Harvard and Oak Ridge except for the placement of a degrader in the Harvard 168 MeV proton beam for improved uniformity. The degrader degraded the particle energy to approximately 128 MeV. To obtain good intensity definition, the beam cross section was collimated to approximately 4.0 square centimeters. A specially designed thin-window ion chamber located between the beam exit port and target was calibrated with a Faraday cup and served to monitor beam current. Energy loss due to the ion chamber at 22 MeV was much less than the ±2 MeV variation associated with the cyclotron. A current integrator monitored the ion chamber current and gave a direct measure of integrated flux.

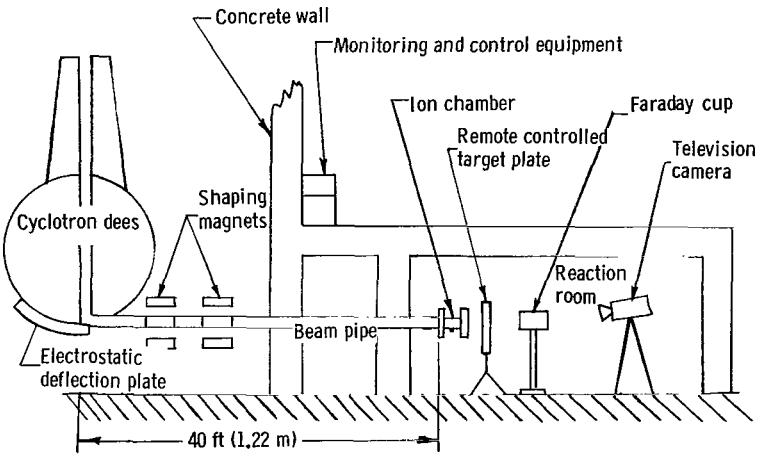

Figure 1.- Test setup in ORNL 86-inch (2.18 m) cyclotron.

A photograph of the transistor mounting apparatus is shown in figure 2. The individual transistors were attached to an aluminum plate perforated to permit passage of the beam. The plate which was fixed normal to the beam was positioned by a remote-control device which alined the desired transistor. A silver activated zinc sulphide phosphor, mounted in one of the perforations, proved adequate for location of the beam. The beam

contour was marked on the screen of a closed-circuit television monitor and the transistor under observation was positioned in the resulting profile. Beam alinement was inspected periodically with the phosphor. Also, terminal strips at each open port provided for external monitoring of the transistors.

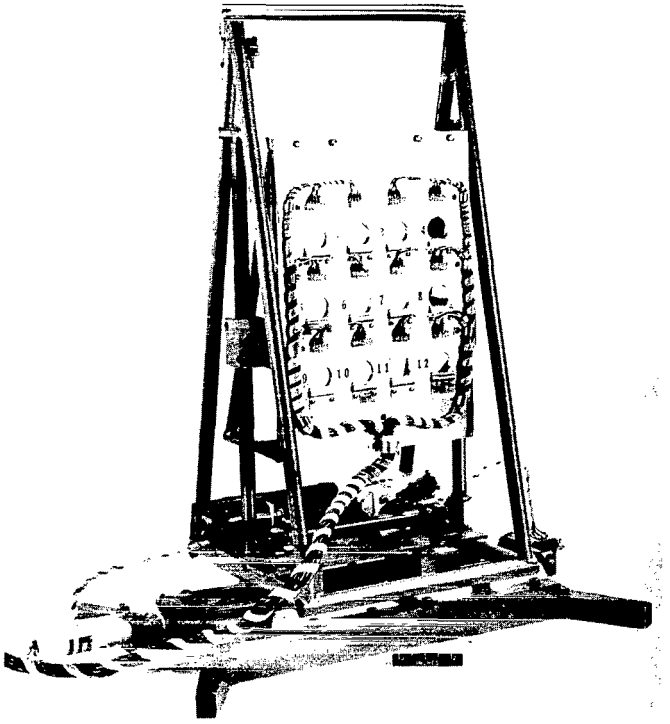

Figure 2.- Transistor mounting apparatus. L-64-677

Transistors were operated at room temperature in both active and inactive circuits to determine the effect of bias voltages on permanent damage. Difficulties with induced currents in the cabling and devices made it necessary to interrupt the proton beam while measurements were obtained at different flux levels.

The parameters I_{DGO}, I_{SGO}, g_m, V_P, I_{DSS}, I_{GSS}, y_{is}, and BV_{DGO} were determined at the NASA Langley Research Center prior to and subsequent to bombardment. A transistor curve tracer and oscilloscope camera displayed and recorded the common-source drain characteristics at various levels of integrated flux. An example of a set of characteristic curves is shown in figure 3. From these photographs the drain-current gate-voltage transfer characteristics may be obtained. Figure 4 gives a typical example of the drain-current gate-voltage transfer characteristics.

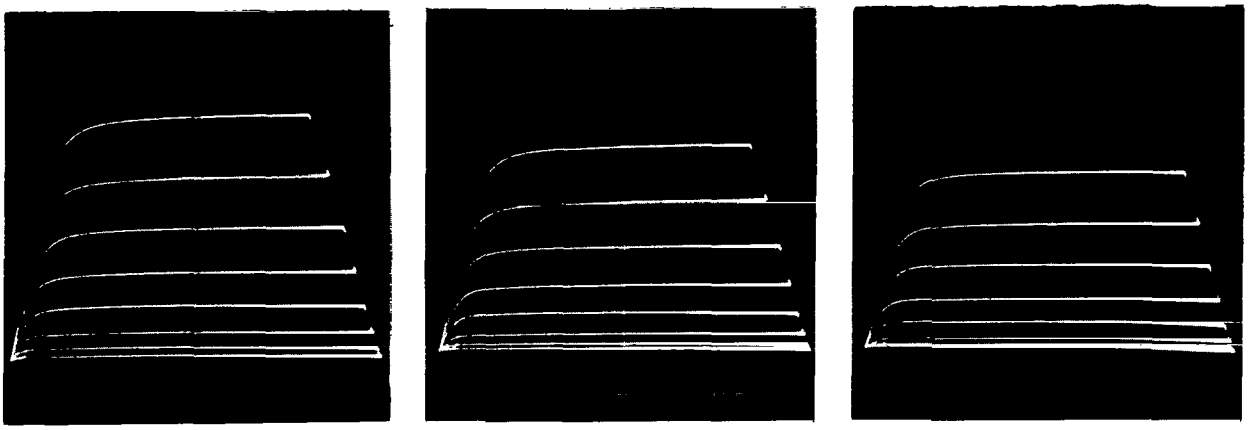

(a) 0 protons/cm^2. (b) 10^{12} protons/cm^2. (c) 2×10^{12} protons/cm^2.

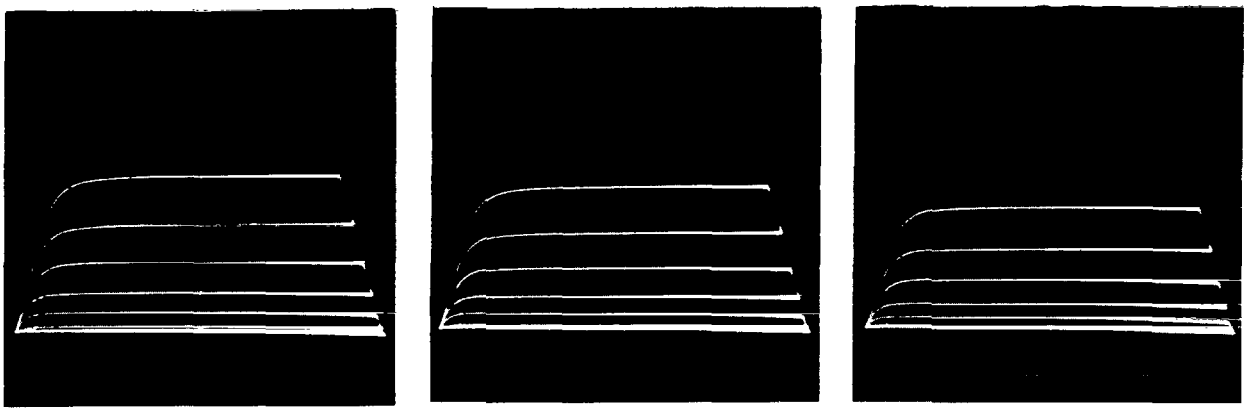

(d) 3×10^{12} protons/cm^2. (e) 4×10^{12} protons/cm^2. (f) 6×10^{12} protons/cm^2.

Figure 3.- Common-source drain characteristics of a type-C p-channel silicon field-effect transistor irradiated with 22 MeV protons to various levels of integrated flux. Scales: V_{DS} = 0.5 volt/div (horizontal); I_{DS} = 0.1 mA/div (vertical); V_{GS} = 0.1 volt/step.

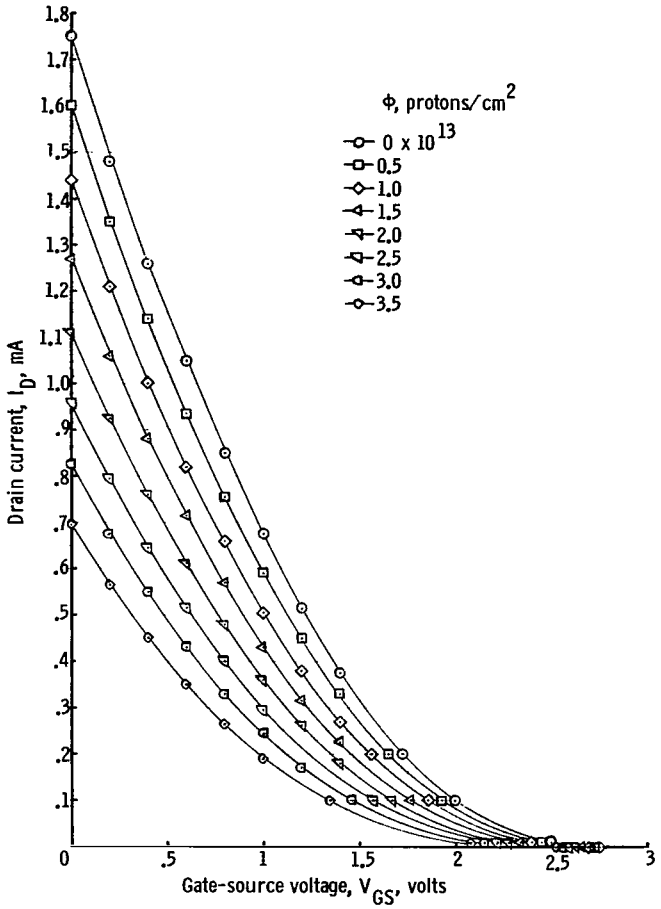

Figure 4.- Gate-voltage drain-current transfer characteristics. Transistor type E. V_D = 10V.

DISCUSSION OF THEORY

The modifications of the idealized theory and experimental models (refs. 6 and 7) along with Shockley's original theoretical treatment (ref. 8) of the field-effect transistor are discussed at length in the literature.

Figure 5 illustrates the basic unipolar field-effect transistor configuration and polarity convention (unipolar, since the device action essentially involves one type of carrier in contrast to the conventional transistor which, in this nomenclature, is called a bipolar structure). The field-effect transistor, conveniently called FET, shown in figure 5 essentially consists of a homogeneously doped n-type rectangular shaped slab of semiconductor with ohmic contacts at each extremity called the drain and source. On two opposite faces of the slab are very heavily doped (high conductivity) p-type regions which form p-n junctions with the n-type semiconductor. Ohmic contact made to the p-type region is called the gate.

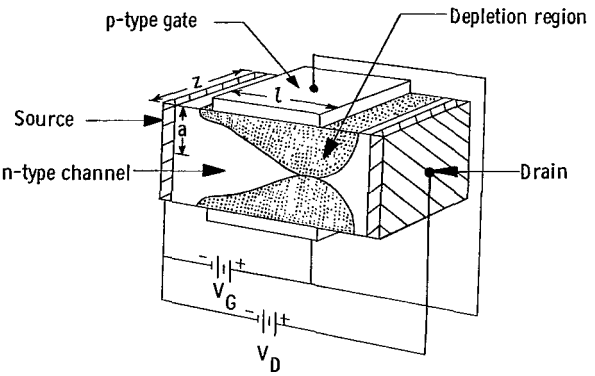

Figure 5.- Structure of basic field-effect transistor.

If the p-n junction is reverse biased, as shown in figure 5, a depletion region forms which is almost entirely free of mobile carriers extending into the n-type slab. The wedge-shaped portion of the slab (unshaded) available for purposes of ohmic conduction between the source and drain, called the channel, is thus reduced in area, and the conductance of this channel is decreased. In fact, then, the FET functions as a conductance modulating device capable of amplification, the volt-ampere characteristic curves of which are similar to those of a pentode vacuum tube. Of course, actual fabricated FET's will have geometries in variance with the simple model treated here but the concept of a well-defined channel remains.

With the geometry and channel conductivity of the FET shown in figure 5, if the wedge-shaped channel narrows slowly enough, the drain current I_D and the mutual transconductance g_m (both per unit channel width) are given analytically as

$$I_D = \frac{1}{l}\left[J(V_D - V_G) - J(V_S - V_G)\right] \tag{1}$$

and

$$g_m = \left(\frac{\partial I_D}{\partial V_G}\right)_{V_D=\text{Constant}} = \left(\frac{2\sigma a}{l W_o^{1/2}}\right)\left[(V_D - V_G)^{1/2} - (V_S - V_G)^{1/2}\right] \tag{2}$$

where

$$J(V) = 2\sigma a V\left[1 - \frac{2}{3}\left(\frac{2KV}{\rho a^2}\right)^{1/2}\right]$$

K dielectric constant

σ channel conductivity

ρ channel donor charge density

W_o $\frac{\rho a^2}{2K}$ (W_o is the bias voltage required between the gate and channel to produce a space charge region of thickness a)

$V_D - V_G \leqq W_o$

$V_S - V_G \leqq W_o$

Equations (1) and (2) also hold for a p-type channel device by replacing ρ by $-\rho$ and hence W_o by $-W_o$.

A typical mode of operation is in a grounded source arrangement. With this assumption, it is clear that the small signal drain conductance

$$g_d = \left(\frac{\partial I_D}{\partial V_D}\right)_{V_G=\text{Constant}} \quad \text{vanishes at} \quad V_D - V_G = W_o$$

For

$$V_D - V_G \geqq W_o$$

the FET is said to operate in the pinch-off region; this condition indicates that the depletion region has penetrated the entire n-type slab somewhere near the drain and leaves an almost zero channel thickness. Thus there will be no further increase in drain current for increasing drain voltage past the vanishing point of $\left(\frac{\partial I_D}{\partial V_D}\right)_{V_G=\text{Constant}}$.

To obtain grounded source analytical expressions for I_D and g_m in the pinch-off region, where operation in most applications appears, the relation $V_D - V_G = W_o$ is applied to equations (1) and (2) and yields

$$I_D = \left(\frac{g_{m,0} W_o}{3}\right)\left[1 + \left(\frac{V_G}{W_o}\right)\left(3 - 2\sqrt{\frac{-V_G}{W_o}}\right)\right] \tag{3}$$

$$g_m = g_{m,0}\left[1 - \left(\frac{-V_G}{W_o}\right)^{1/2}\right] \tag{4}$$

where

$$g_{m,0} = \frac{2\sigma a}{l}$$

An approximate power-law relation based on a charge control model has been obtained for the FET (refs. 9 and 10) for pinch-off operation and is given by

$$I_D = \frac{\mu Q_c^{\,2}}{2l^2 C_g}\left(1 + \frac{V_G}{Q_c/C_g}\right)^2 \tag{5}$$

which results in the expression for transconductance

$$g_m = \frac{\mu Q_c}{l^2}\left(1 + \frac{V_G}{Q_c/C_g}\right) \tag{6}$$

where

Q_c mobile charge which would exist in the absence of the gate

V_P Q_c/C_g equals pinch-off voltage corresponding to W_o in ideal theory

C_g a capacitance approximately constant for $V_D > V_P$.

Commercial FET's have been found to obey such a square law (eq. (5)) reasonably well and with more accuracy than the theory of the ideal case.

For obvious reasons the voltage-ampere and transconductance equations (eqs. (3), (4), (5), and (6)) become more readily amenable to analysis if the gate voltage V_G is maintained at a zero level. The simplified expressions for equations (3) to (6) are then

$$(I_D)_{V_G=0} = I_{DSS} = \frac{g_{m,0}W_o}{3} = \left(\frac{a^3}{lK}\right)\mu\rho^2 \tag{7}$$

$$(g_m)_{V_G=0} = g_{m,0} = \left(\frac{2a}{l}\right)\mu\rho \tag{8}$$

$$I_{DSS} = \frac{\mu Q_c^{\,2}}{2l^2 C_g} \tag{9}$$

$$g_{m,0} = \frac{\mu Q_c}{l^2} \tag{10}$$

Further, if the assumption (which may be omitted, as shown subsequently) is made that the mobile charge Q_c which exists in the absence of the gate is proportional to the mobile charge density (which implies a homogeneous impurity distribution as assumed in an ideal case), then the relations (7), (8), (9), and (10) are equivalent and may be represented by

$$I_{DSS} = C_1 \mu \rho^2 \tag{11}$$

$$g_{m,0} = C_2 \mu \rho \tag{12}$$

where C_1 and C_2 depend on the geometry of the transistor.

It is desirable to predict the degradation of the electrical parameters of the field-effect transistor in a known radiation (proton) environment. Even when the complete physical parameters are known, an accurate description of the behavior of the device itself is not simple. The comparison of experimental results with the preceding volt-ampere and transconductance expressions is briefly considered herein.

The semipermanent damage induced in the bulk of a semiconductor is in the form of lattice defects caused by the displacement of atoms within the crystal. These defects comprise interstitial atoms, their vacated sites (called vacancies), and various interacting complexes such as di-vacancies and vacancy-impurity atom combinations. The creation of these defects has the electrical consequence of the introduction of energy levels in the forbidden gap of the semiconductor which behave as donor and acceptor states and recombination centers. Allowed energy levels in the forbidden energy gap will alter the mobile carrier concentration and, depending on their charge state, function as scattering centers which reduce the carrier mobility.

An approximate relation (refs. 1 and 2) between carrier concentration (or carrier charge density) and energetic particle flux is given by

$$\rho = \rho_o + \left(\frac{d\rho}{d\phi}\right)_o \phi \tag{13}$$

where

$\frac{d\rho}{d\phi}$ is constant in region of interest

ρ_o initial carrier charge density

ϕ particle flux density

$$\left(\frac{d\rho}{d\phi}\right)_o = q\left(\frac{dn}{d\phi}\right)_o = q(\text{Initial carrier density removal rate})$$

In the approximation the following restrictions are assumed: (1) the Fermi level does not change its position in the forbidden energy gap as the concentration of donor and acceptor defect levels increases and (2) the semiconductor material is thin enough that the energy of the assumed monoenergetic radiation does not significantly degrade in passing through it since $\left(\frac{d\rho}{d\phi}\right)_o$ is energy dependent.

The Fermi level, however, will begin to shift with the changing conductivity under extended particle bombardment in such a way as to decrease the fractional filling of the pertinent acceptors or donors. The carrier concentration then drops less rapidly than is indicated by equation (13). The linear dependence of carrier concentration on flux appears to hold well up to conductivities reduced to one-half their initial values.

The condition that the mobile charge Q_c which exists in the absence of the gate is homogeneously distributed needs to be relaxed. To illustrate the argument, it is necessary to note that the initial carrier removal rate $\left(\frac{dn}{d\phi}\right)_o$ is indeed a function of mobile carrier density in addition to particle energy. Therefore, since ρ_o is a function of the position vector $\bar{x}$ then

$$\rho_o = \rho_o(\bar{x})$$

and

$$\left(\frac{d\rho}{d\phi}\right)_o = f\left(\rho_o(\bar{x})\right)$$

Finally, Q_c is found to be

$$Q_c(\phi) = \int \rho(\phi)\, d^3x = \int \rho_o(\bar{x})\, d^3x + \phi \int f\left(\rho_o(\bar{x})\right) d^3x$$

where the integration is over the channel volume for zero gate voltage or

$$Q_c(\phi) = (Q_c)_o + \phi\left(\frac{dQ_c}{d\phi}\right)_o \tag{14}$$

Although equation (13) gives the intensive function ρ as a function of ϕ, it is also valid for Q_c except for the different initial carrier removal rate in equation (14). Equation (14) then makes equations (9) and (10) immediately compatible with equations (11) and (12).

Since the carrier mobility degradation is usually small compared with carrier concentration decreases, equation (13) can be combined with equations (11) and (12) to yield the particle flux dependencies of the zero-gate voltage drain current and transconductance

$$I_{DSS} = (I_{DSS})_o(1 + \gamma\phi)^2 \tag{15}$$

$$g_{m,0} = (g_{m,0})_o(1 + \gamma\phi) \tag{16}$$

where

$$\gamma = \frac{1}{\rho_o}\left(\frac{d\rho}{d\phi}\right)_o = \frac{1}{n_o}\left(\frac{dn}{d\phi}\right)_o$$

A linear expression similar to equation (16) also holds for the pinch-off voltage V_P or W_O. Unfortunately, it is not possible to measure directly the pinch-off voltage accurately because of the asymptotic tendency of the drain current to its leakage level for increasing (absolute magnitude) gage voltage and the lack of possibility of constructing straight-line intercepts. Therefore equations (15) and (16) will be compared with experimental results.

RESULTS AND DISCUSSION

The topics brought out in the section entitled "Discussion of Theory" are briefly compared with experiment in the present section, and various results of the irradiation tests are discussed.

In order to recall the approximate technique for obtaining the zero-gate-voltage transconductance refer to figure 4 which shows a typical set of transfer characteristics (in particular, for transistor type E) with integrated proton flux as a parameter. Figure 4 shows that the small-signal zero-gate-voltage transconductance (the slope of the characteristic curves) exceeds the transconductance computed from a finite increment (0.2 gate volt for type E). Tolerance of this error is momentarily accepted and is assumed to be small.

Since it is expected that $g_{m,0}$ should more closely follow a linear variation with flux than does drain current, the rule of least squares is applied to the curves of the variation of $g_{m,0}$ with ϕ. For illustrative purposes, three transistor types, all bombarded with 22 MeV protons, were examined in sufficient detail for these determinations. Types E and C possess $g_{m,0}$ variations in reasonable accord with the anticipated first-degree dependence. In contrast to equation (15), the curves for the variation of drain current with ϕ for type A nicely adapt to a straight-line fit. The results are:

for type E,

$$\frac{g_{m,0}}{(g_{m,0})_o} = \left(1 - 0.148 \times 10^{-13}\phi\right) \tag{17}$$

for type C,

$$\frac{g_{m,0}}{(g_{m,0})_o} = 0.99\left(1 - 0.0737 \times 10^{-13}\phi\right) \tag{18}$$

and for type A,

$$\frac{I_{DSS}}{(I_{DSS})_o} = \left(1 - 0.186 \times 10^{-13}\phi\right) \tag{19}$$

where ϕ is in protons/cm^2. These equations are plotted as solid lines in figures 6, 7, and 8.

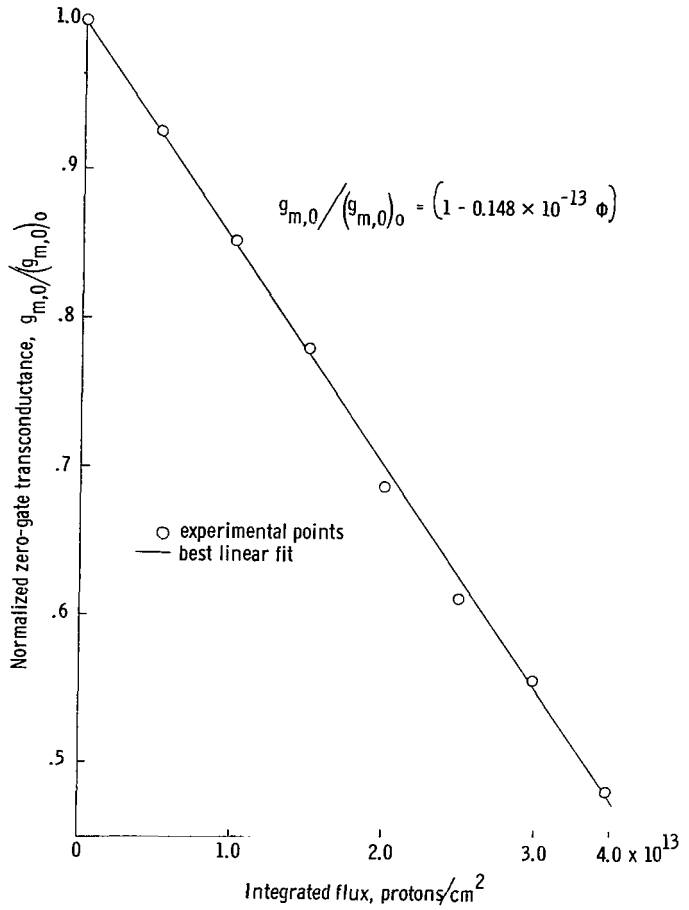

Figure 6.- Normalized zero-gate transconductance as a function of 22 MeV proton flux for transistor type E (n-channel).

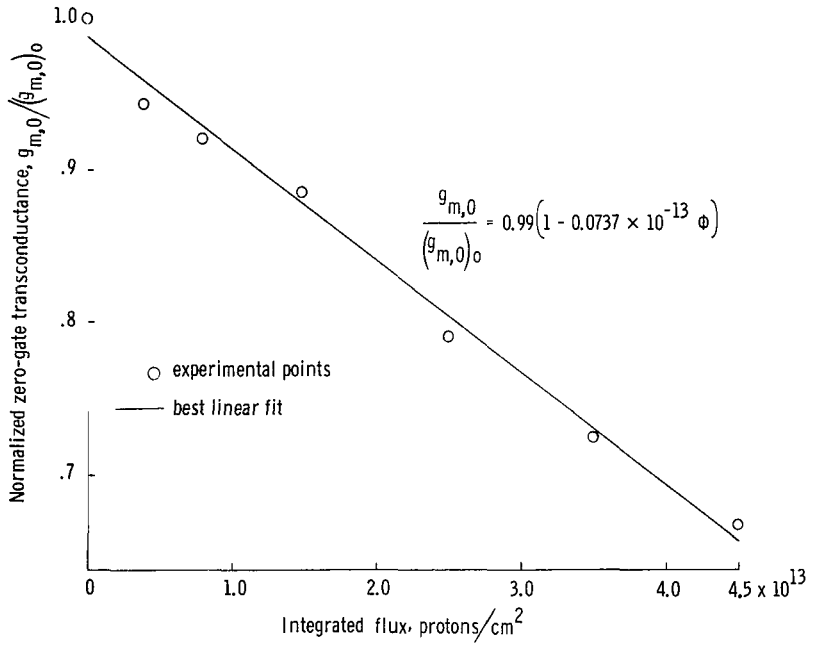

Figure 7.- Normalized zero-gate transconductance as a function of 22 MeV proton flux for transistor type C (p-channel).

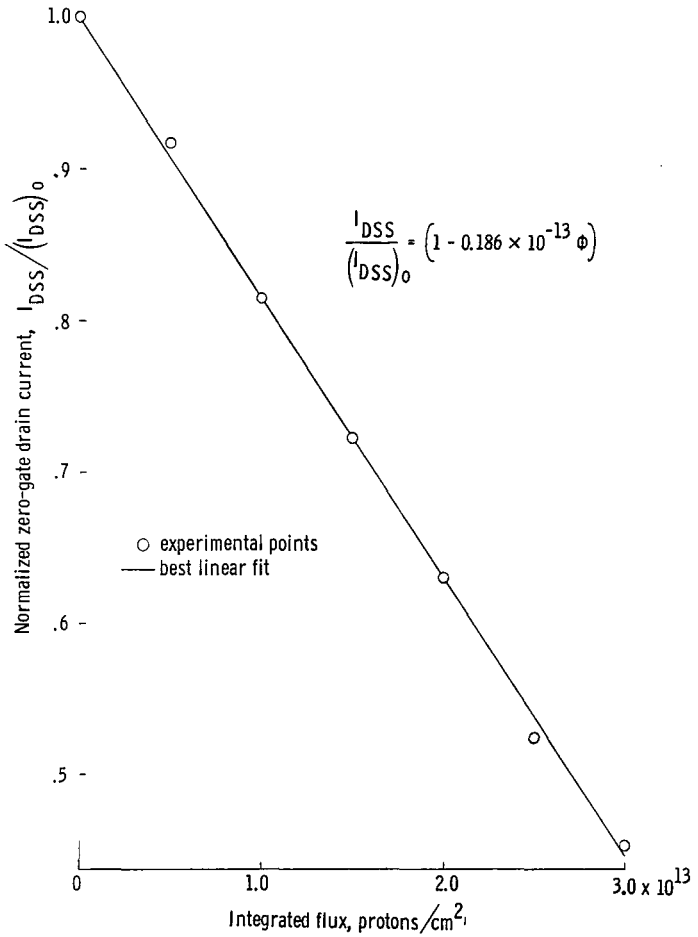

Figure 8.- Normalized zero-gate drain current as a function of 22 MeV proton flux for transistor type A (n-channel).

Equation (9) normalized and in terms of carrier concentration is

$$\frac{n}{n_o} = \left[1 + \frac{1}{n_o}\left(\frac{dn}{d\phi}\right)_o \phi\right] \tag{20}$$

By associating this linear variation in ϕ with the normalized transconductance expressions of equations (17) and (18) and the normalized drain current relation of equation (19), it may be concluded that the coefficients of the flux (neglecting the near unity multiplying constants) should correspond numerically to that in equation (20) which was obtained from experimental observations on the basic semiconductor material. Of course, associated with this comparison is a difficulty stated previously concerning the impreciseness of some of the physical parameters of the device. Without reference to any transistor specifications, it is interesting to make rough comparisons between the material and device carrier removal rates.

Transistor types E and A are silicon planar n-type devices and type C has a p-type channel conductivity. Assume as a representative value that the channel region (before irradiation) is of 10 Ω-cm silicon. It has been observed that average initial carrier removal rates under 17 MeV proton bombardments for 10 Ω-cm silicon are:

for n-type,

$$\left(\frac{dn}{d\phi}\right)_o = -7.6$$

and for p-type,

$$\left(\frac{dn}{d\phi}\right)_o = -13$$

Here, the results for 17 MeV irradiation are considered valid, since 22 MeV protons suffer an energy loss of approximately 5 MeV while penetrating the 10 to 15 mil copper transistor enclosures. Therefore, the device removal rates are:

for type E, n-type,

$$n_o\gamma = -7.4$$

for type C, p-type,

$$n_o\gamma = -7.4$$

and for type A, n-type,

$$n_o\gamma = -9.3$$

This roughly good agreement gives more indication that $g_{m,0}$ does indeed vary proportionally with carrier concentration for types E and C and, more unexpectedly, that I_{DSS} changes linearly with carrier concentration for type A.

Equations (15) and (16) indicate a square-law dependence of drain current on transconductance for the parametric variable ϕ given by

$$\frac{I_{DSS}(\phi)}{(I_{DSS})_o} = \left[\frac{g_{m,0}(\phi)}{(g_{m,0})_o}\right]^2 \tag{21}$$

It is found that the exponent 2 must be replaced by an arbitrary constant, for example, C_4, to preserve the power-law nature of the I_{DSS} and $g_{m,0}$ relationship which may be represented as

$$\frac{I_{DSS}(\phi)}{(I_{DSS})_o} = C_3\left[\frac{g_{m,0}(\phi)}{(g_{m,0})_o}\right]^{C_4} \tag{22}$$

where C_4 seems to satisfy the inequality $1 < C_4 < 2$ and C_3 is near unity.

Again, the same three transistor types serve to demonstrate experimental findings for C_4. Figure 9 shows logarithmic plots of transconductance as a function of drain current for transistor types E, C, and A, respectively. The solid line in each figure corresponds to the least-squares fit of the data in the logarithmic scale. Good statistical agreement obtains for type E and to a lesser extent in types C and A. The slopes of these curves specify C_4 as

1.27 for type E
1.60 for type C
1.35 for type A

There is no clear inclination for C_4 to assume values near 2.

In the section entitled "Discussion of Theory," it was noted that an ideal linear expression similar to that for transconductance, given by equation (16), also holds for the pinch-off voltage but that straightforward measurement of this parameter is not easy. However, an indirect method of obtaining the pinch-off dependence on proton flux should be possible.

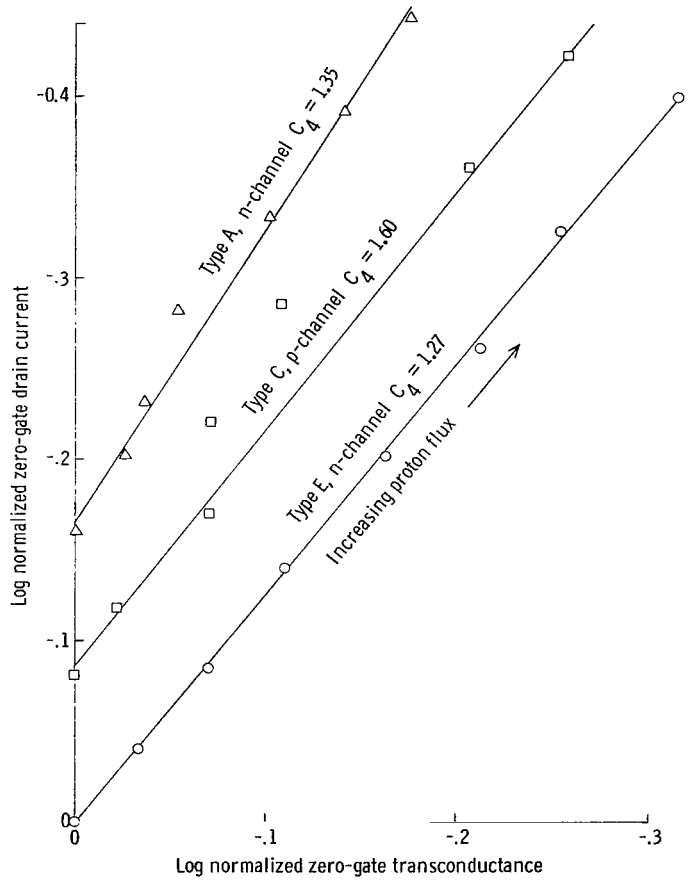

Figure 9.- Log normalized zero-gate drain current as a function of log normalized zero-gate transconductance for 22 MeV proton bombardment.

Rewriting equations (3) and (5) in the form

$$I_D = I_{DSS}\left[1 + \left(\frac{V_G}{V_P}\right)\left(3 - 2\sqrt{\frac{-V_G}{V_P}}\right)\right] \tag{23}$$

$$I_D = I_{DSS}\left(1 + \frac{V_G}{V_P}\right)^2 \tag{24}$$

where W_0 in equation (3) is replaced by V_P, and differentiating with respect to V_G to find the zero-gate-voltage transconductance equations

$$g_{m,0} = \frac{3I_{DSS}}{V_P} \tag{25}$$

and

$$g_{m,0} = \frac{2I_{DSS}}{V_P} \tag{26}$$

then equations (25) and (26) are equivalent to the simple form

$$g_{m,0} = \frac{C_5 I_{DSS}}{V_P}$$

Previous results for the variations of $g_{m,0}$ and I_{DSS} with proton flux indicate that the pinch-off voltage as a function of particle flux is expressed by

for type E,

$$V_P = (V_P)_0\left(1 - 0.148 \times 10^{-13}\phi\right)^{0.27}$$

for type C,

$$V_P = (V_P)_0\left(1 - 0.0737 \times 10^{-13}\phi\right)^{0.6}$$

for type A,

$$V_P = (V_P)_0\left(1 - 0.186 \times 10^{-13}\phi\right)^{0.35}$$

These functional relations for V_P are obviously not linear with flux. The somewhat reduced damage rate of V_P found here is similar to that which would be obtained by projecting the very rough assumption of measuring the pinch-off voltage by the indication of gate-source voltage for a fixed, exceedingly low, drain current. Figure 4 exemplifies the effect of the "crowding" of the parametric curves at small drain currents, which gives rise to smaller apparent changes in pinch-off voltage.

The behavior of the pinch-off voltage with particle flux may be substantiated by an experiment in which drain current and small signal transconductance are recorded as functions of gate voltage with flux as a parameter. This information would enable the approximate calculation of the pinch-off voltage and power-law exponent based on the charge control model (refs. 9 and 10). Equation (5) in its most general form has an exponent n, instead of 2. Differentiation of this modified form of equation (5) to obtain transconductance gives:

$$\frac{I_D(\phi)}{g_m(\phi)} = \frac{1}{n}\left[V_P(\phi) + V_G\right] \tag{27}$$

Therefore, by plotting the ratio of drain current to transconductance as a function of gate voltage, the pinch-off voltage corresponding to each proton flux level can be calculated from the resulting linear graph.

In the following discussion an attempt is made to account for the apparent deviations from the theory.

Perhaps significant, in reference to the charge control model, the mobile charge Q_c which would exist in the absence of the gate is not uniformly distributed in such devices as planar FET's. In addition, there are complex junction impurity doping profiles. Although the charge control equations (5) and (6) are written independently of impurity profile, it has been implicitly assumed in their presentation that a constant channel electric field exists. However, this assumption is not really valid and the zero-gate drain current and transconductance immediately become functions of the specific transistor geometry over and above the somewhat restrictive one dimensionality of the FET model. Moreover, the carrier mobility is a mild function of doping concentration upon which the average transit time for the carriers in the channel depends. The preceding statements are independent of the justification given by equation (14) that Q_c varies linearly with proton flux despite inhomogeneous doping since the application of this result to equations (9) and (10) implies nothing about mobility.

Also, it should be recalled that equations (1) and (2), describing the ideal FET model, are based on a homogeneously doped semiconductor slab. Deviations in geometry and homogeneity will modify these equations and the zero-gate drain current and transconductance dependences on particle flux.

Other sources of theoretical disagreement may be flux monitoring errors which possibly range up to ±10 percent and the finite incremental method of transconductance measurement previously discussed. An indirect effect due to a portion of the channel between the source and gate unmodulated by the gate potential may be seen in the

measured transconductance. The degenerative effect of this channel resistance R_S arises as an apparent measured transconductance (here, zero-gate transconductances), $g'_{m,0}$, given by

$$g'_{m,0} = \frac{g_{m,0}}{1 + R_S g_{m,0}}$$

where $g_{m,0}$ is the true active channel zero-gate transconductance. If it is assumed that $g_{m,0}$ and $(1/R_S)$ have the linear variations with flux, $g_{m,0} = (g_{m,0})_o(1 + \gamma_1\phi)$ and $(1/R_S) = (1/(R_S)_o)(1 + \gamma_2\phi)$, then the apparent transconductance $g_{m,0}$ will degrade with particle flux more rapidly or less rapidly than the true transconductance, since the denominator, $1 + R_S g_{m,0}$ also increases or decreases with ϕ as $\gamma_1 < \gamma_2$ or $\gamma_1 > \gamma_2$. Inhomogeneous doping may prevent the condition where $\gamma_1 = \gamma_2$. The resistance R_S is usually minimized for a commercial FET, but with significant decreases in channel conductivity, degeneration may be induced by the extended particle bombardment.

Several miscellaneous results can now be discussed and the proton irradiation data displayed. The appendix contains plots of normalized zero-gate drain current and transconductance as functions of integrated proton flux for transistor types A, B, C, D, E, F, G, H, and K. (No data were available for transistor type J.) An average of five transistors of each type served to furnish the proton bombardment data for the appendix figures. Since there is spread among the responses of the transistors of a particular type to the damaging radiation, the region of the plots between the maximum and minimum data points is shown crosshatched as an alternative to individual maps of each device or a single curve representing the average value of the electrical parameter. However, the average of the responses of the transistors of a particular type usually falls in the center of the crosshatched domain. These plots should project reasonably well the expected proton irradiation results of an even larger group (of each type) of commercial FET's.

One cause of the transistor variations, which results in rather excessive scatter in radiation response noted in many of the FET's originates from unwanted impurities remaining in the semiconductor material after manufacturing processes. The damage to the semiconductor crystal (carrier removal rate) is a sensitive function of these impurities, and the concentration of the impurities is not very well controlled. Also, flux monitoring errors and initial design variations and differences may introduce significant divergence.

An example which illustrates some expected features of the proton bombardments is shown in figure 10 which is a plot of zero-gate drain current as a function of integrated proton flux for transistor types H and J. Type H, a p-channel silicon planar FET, has been irradiated with 22 MeV and 128 MeV protons. From figure 10, it is observed that

the transistor experiences more extensive degradation in drain current under bombardment with 22 MeV protons than with 128 MeV protons. The range of 17 MeV protons is much greater than the thickness of the semiconductor crystal, as is suggested from theory since the scattering cross section (elastic scattering) for 22 MeV protons is greater than that for 128 MeV protons. Then the number of primary lattice displacements per unit distance along the track of an incident 22 MeV proton exceeds that of the 128 MeV proton, and the channel carrier concentration correspondingly undergoes more change.

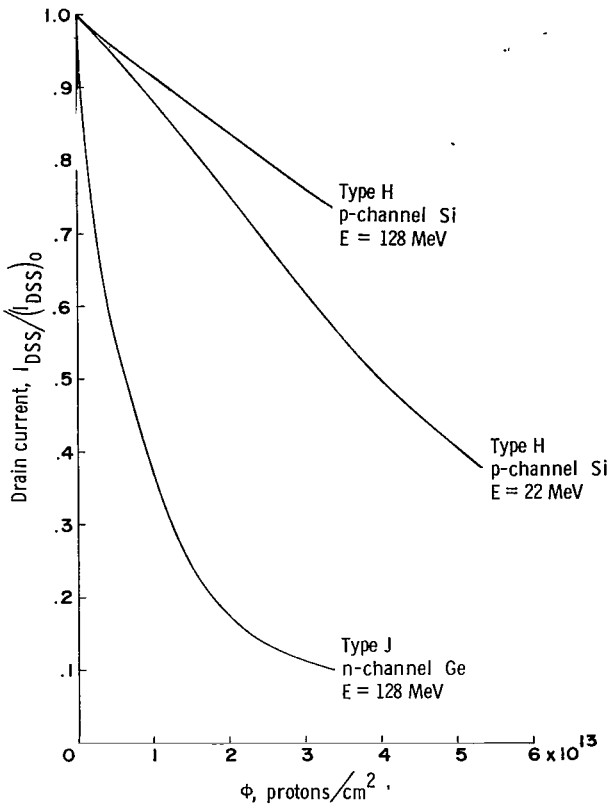

Figure 10.- Zero-gate drain current as a function of integrated proton flux.

Transistor type J, an n-channel germanium alloy junction FET, has been subjected to 128 MeV protons. Notice in figure 10 that the drain current of type J degrades more than an order of magnitude more rapidly than the silicon p-channel FET, type H. However, in comparing one transistor with another of a different type, namely type J to type H, it must be insured that the comparison is qualified. Without any knowledge of the channel resistivities of the two transistors, it will be noted that carrier removal rates are higher in n-type germanium materials than in n- or p-type silicon materials for materials of the same conductivity and typical FET fabrication channel conductivity ranges. Indeed, for 10 ohm-cm semiconductors the carrier removal rate of n-type germanium materials is roughly a factor of 20 times greater than either n- or p-type silicon materials. Perhaps, then, it is reasonable to speculate that the previous statements offer one explanation for the higher radiation sensitivity of the germanium type-J FET. Unfortunately, a meaningful degradation curve for type-J FET's under 22 MeV protons bombardment for comparison to 128 MeV proton response, as demonstrated in type-H FET's, was not obtainable. This effect was a consequence of a silicon potting material of thickness near the range of the protons in the substance. Proton fluxes capable of inflicting displacement damage on the semiconductor crystal of the device are sizably reduced, and the apparent radiation resistance of the FET to 22 MeV protons increases.

The following table gives the integrated proton flux range and energy necessary to cause 30 percent degradation in zero-gate drain current for the FET's. Some exceptions noted in the table indicate the dispersion in percent degradation for a particular flux, since 30 percent degradation was not achieved in the existing experimental procedure. The table also exhibits the integrated proton flux needed to cause 30 percent degradation in zero-gate transconductance.

Transistor type	Proton energy, MeV	Proton flux necessary to cause 30% degradation in I_{DSS}, protons/cm^2	Degradation at indicated flux, %	Proton flux necessary to cause 30% degradation in g_m, protons/cm^2	Degradation at indicated flux, %
A	22	$3.4 \pm 1.6 \times 10^{12}$	30	$4.5 \pm 2.5 \times 10^{12}$	30
B	22	8×10^{12}	10 to 30	7×10^{12}	5 to 20
C	22	3.5 ± 1.5	30	$5.3 \pm 1.8 \times 10^{12}$	30
D	22	5.0 ± 3.0	30	$4 \pm 3 \times 10^{12}$	30
E	22	$5.8 \pm 2.3 \times 10^{12}$	30	5.8 ± 2.1	30
F	22	$6.6 \pm 1.4 \times 10^{12}$	12 to 16	8×10^{12}	8 to 12
G	22	$5.0 \pm 2.0 \times 10^{12}$	30	$5.5 \pm 2.5 \times 10^{12}$	30
H	22	$2.3 \pm 1.0 \times 10^{13}$	30	$5.3 \pm 0.2 \times 10^{13}$	30
H	128	3.36×10^{13}	17 to 30	3.36×10^{13}	7 to 15
J	128	$3.0 \pm 1.0 \times 10^{12}$	30	3.36×10^{13}	50
K	22	2×10^{13}	10 to 15	2×10^{13}	7 to 14

The electrical parameters I_{DSS}, I_{GSS}, BV_{DGO}, I_{DGO}, I_{SGO}, V_P, y_{is}, and g_m were determined at Langley Research Center prior and subsequent to bombardment. These pre- and post-irradiation quantities for each device of every transistor type are presented in tables I and II for 128 MeV and 22 MeV protons, respectively.

With few exceptions the pinch-off voltage V_P underwent relatively small changes (absolute value decreases) due to the crowding effect of the transfer characteristics at low drain currents. Of course, V_P has already been shown not to be the true pinch-off voltage but a rough indication of this quantity. However, manufacturer's specifications commonly define V_P as pinch-off voltage, and in a demonstration of irradiation data it is best included among the measured electrical parameters.

The surface may affect the reverse current of a junction in several ways (ref. 11). A grossly contaminated surface may provide a leakage path of very low resistance. Also, a high generation rate at the surface increases the reverse current and may dominate it. Finally, the surface may give rise to more or less abrupt catastrophic increase of current with a well-defined breakdown voltage. Therefore, the magnitude of surface-conditioned reverse currents and breakdown voltages is very sensitive to the state of the

surface and to the composition of the surrounding atmosphere. The more familiar bulk effects of minority carrier lifetime and space charge recombination-generation are also important.

Proton bombardment of a semiconductor surface may have a profound effect on its physical and electrical nature. In addition, a reverse biased junction with a gas atmosphere in ionizing radiation will give rise to inversion layers on the surface at the junction. This "Telstar effect" is not applicable in the case of FET's, since tables I and II list I_{DGO}, I_{SGO}, and I_{GSS} at time intervals large enough after radiation exposure at zero biases to establish equilibrium. Increases in surface contamination (taken to include radiation induced physical changes such as energies of surface states and density redistribution), surface generation rate, and space charge recombination-generation, and decreases in minority carrier lifetime do, however, account for the changes in source- and drain-gate reverse currents. These currents increased from a factor of about 3 up to 10^5 for the various proton flux levels noted in tables I and II.

The variations (increases) in drain-gate breakdown voltage BV_{DGO} were typically small but enlarged by a factor of 3 in some instances. Upon annealing at 200° C for 30 minutes, the breakdown voltages returned to within 10 percent of their initial values. The maximum value of BV_{DGO} which can be achieved in any junction may be attributed to the breakdown of the bulk material of the junction under the action of the high electric field in the space charge region. An empirical expression for this maximum BV_{DGO} is (from ref. 11)

$$BV_{DGO} = C_6\sigma^{-C_7}$$

where

C_6 constant

σ conductivity of channel region

C_7 is less than unity

Therefore, as majority carriers are removed from the channel, σ decreases and BV_{DGO} increases with increasing particle flux. This effect may account partially for the generally observed small increases in BV_{DGO}. The fewer cases of sizable increase were due to changes in surface condition.

In-beam electrical measurements were not made because of the excessive pick-up of spurious signals in the circuitry and cabling. Experiments with minority carrier (injection type) transistors indicate that protective coatings (excluding metal oxides

such as SiO_2) and potting materials possess unstable transient in-beam characteristics. The silicon potting material in the germanium FET enclosures resulted in more pronounced ionization effects in the germanium devices than in the silicon FET's the surfaces of which were dry and in which no filler was used within the can. Appreciable annealing of drain current and transconductance took place in the germanium units at room temperature over a 2-week period subsequent to bombardment. Very little annealing was observed in the silicon FET's probably because of their more stable surface configurations.

CONCLUDING REMARKS

Simple theory from a field-effect transistor model based on initial carrier removal rate indicates a linear and quadratic dependence of zero-gate transconductance and drain current on integrated proton flux, respectively. Two of the three types of field-effect transistors studied in detail possessed zero-gate-transconductance variations in reasonable accord with the anticipated first-degree dependence. In contrast, the curves of zero-gate drain current as a function of flux of the third type adapt well to a straight-line fit. Also, the quadratic dependence of the zero-gate voltage drain current fails, but a power law relation with proton flux holds and the exponents range from 1 to 1.6.

Despite the partial agreement with a theoretical model, accurate radiation damage prediction techniques for the field-effect transistors are not readily obtainable because of the initial spread in irradiation responses of the transistors. On a more favorable note, it was found that many field-effect transistors possess a radiation resistance to 22 and 128 MeV protons at least comparable to most narrow-base minority carrier devices.

Langley Research Center,
National Aeronautics and Space Administration,
Langley Station, Hampton, Va., April 25, 1966,
124-09-01-16-23.

APPENDIX

PLOTS OF NORMALIZED ZERO-GATE DRAIN CURRENT AND TRANSCONDUCTANCE AS FUNCTIONS OF INTEGRATED PROTON FLUX FOR VARIOUS TRANSISTOR TYPES

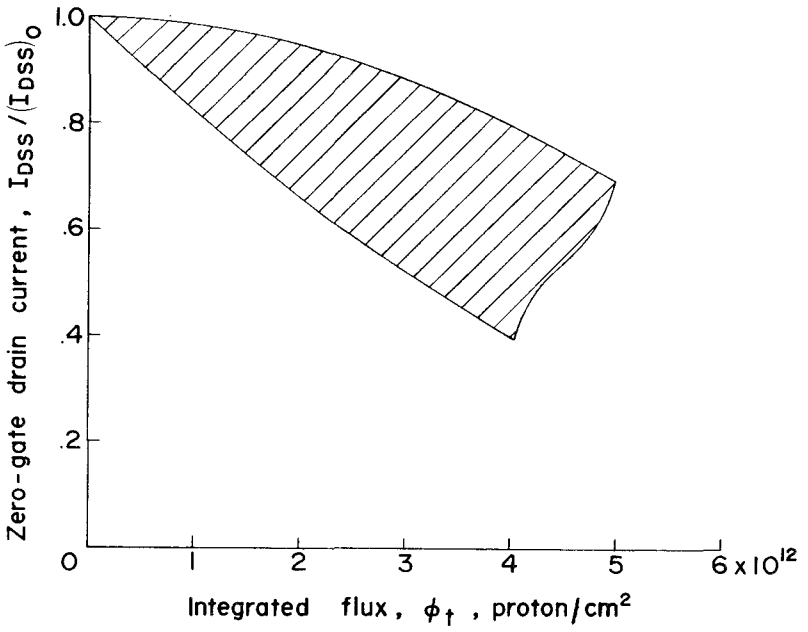

Transistor type A; n-channel Si; planar; proton energy = 22 MeV.

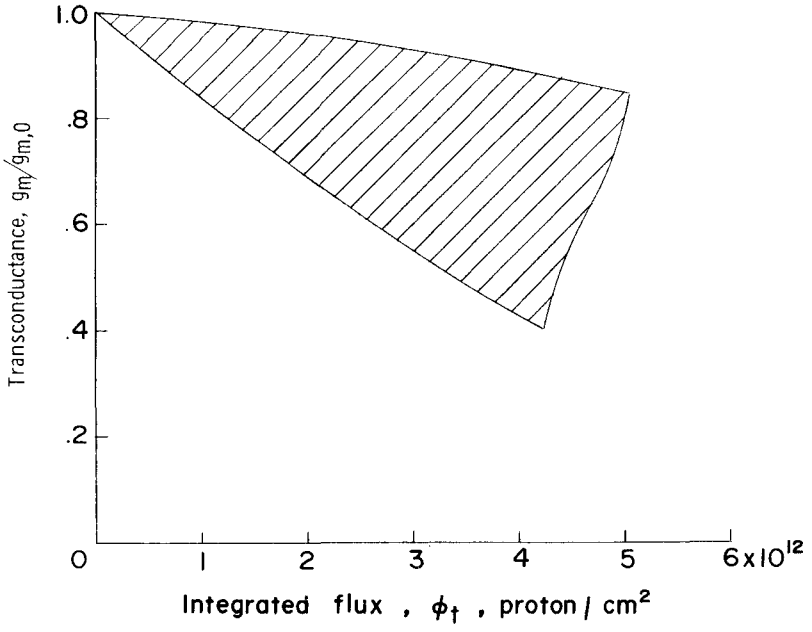

Transistor type A; n-channel Si; planar; proton energy = 22 MeV.

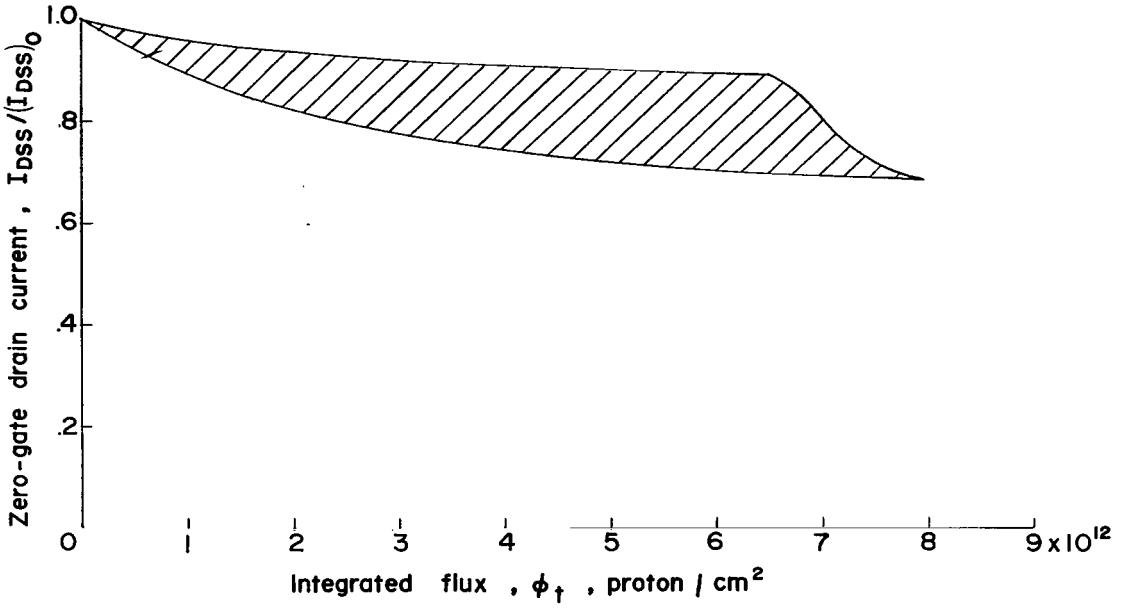

Transistor type B; p-channel Si; diffused junction; proton energy = 22 MeV.

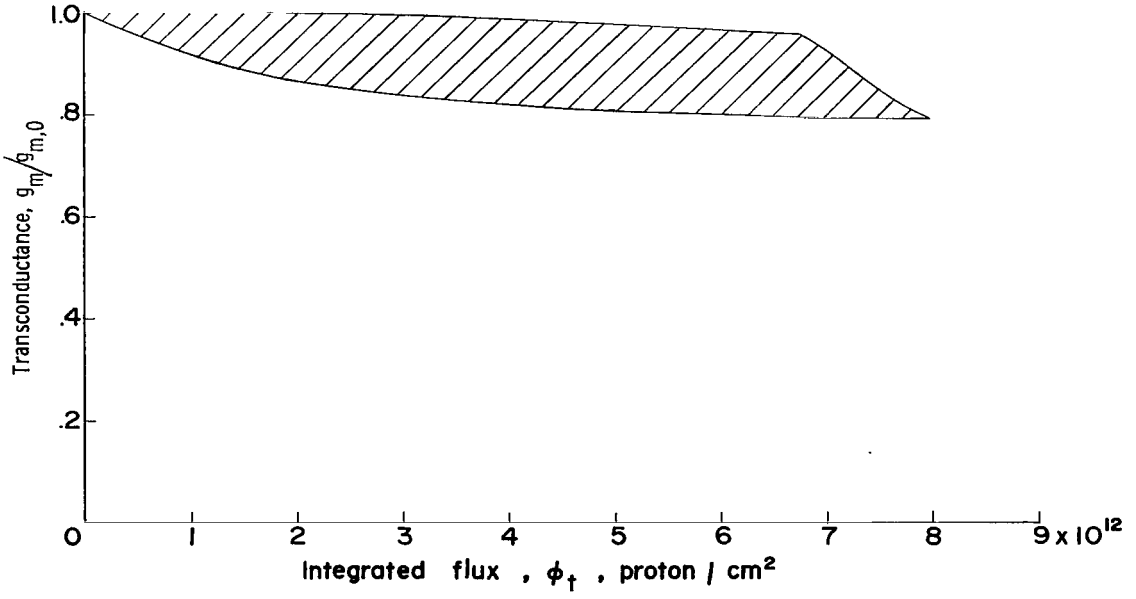

Transistor type B; p-channel Si; diffused junction; proton energy = 22 MeV.

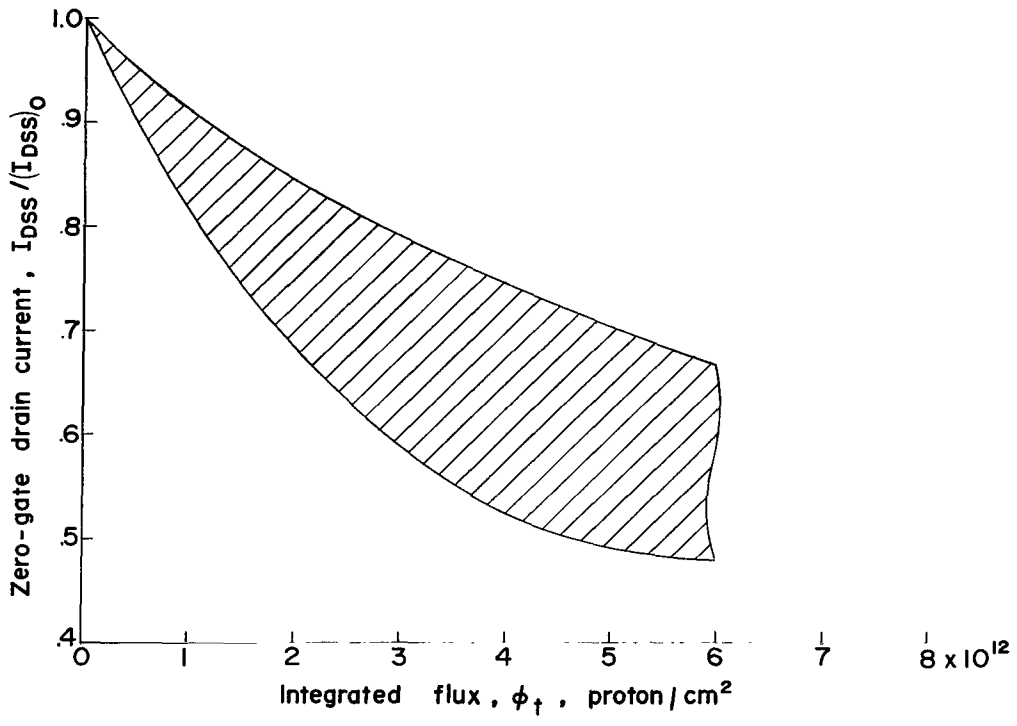

Transistor type C; p-channel Si; planar diffused junction; proton energy = 22 MeV.

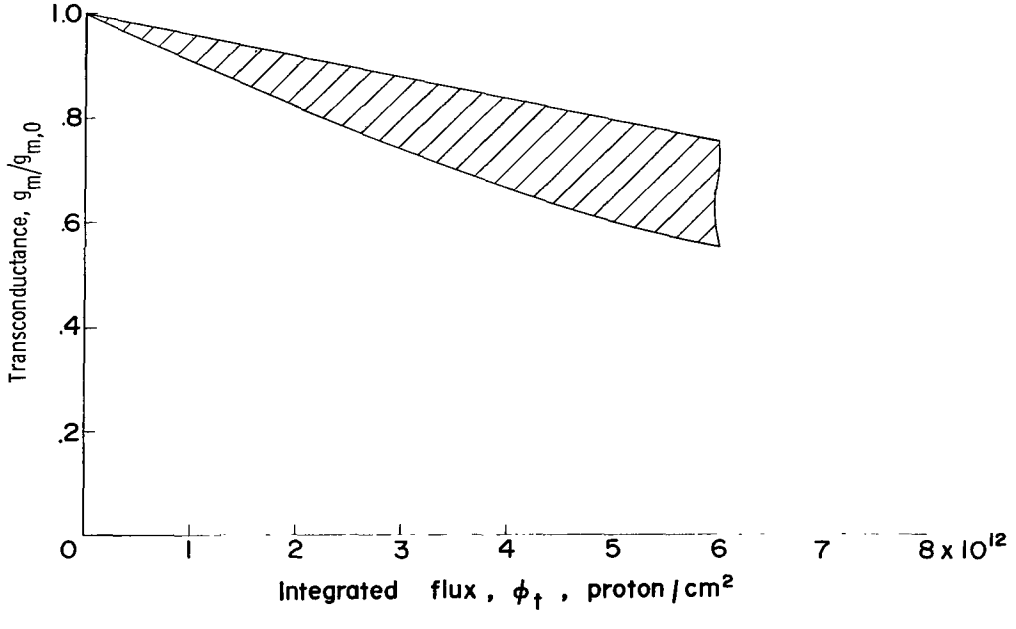

Transistor type C; p-channel Si; planar diffused junction; proton energy = 22 MeV.

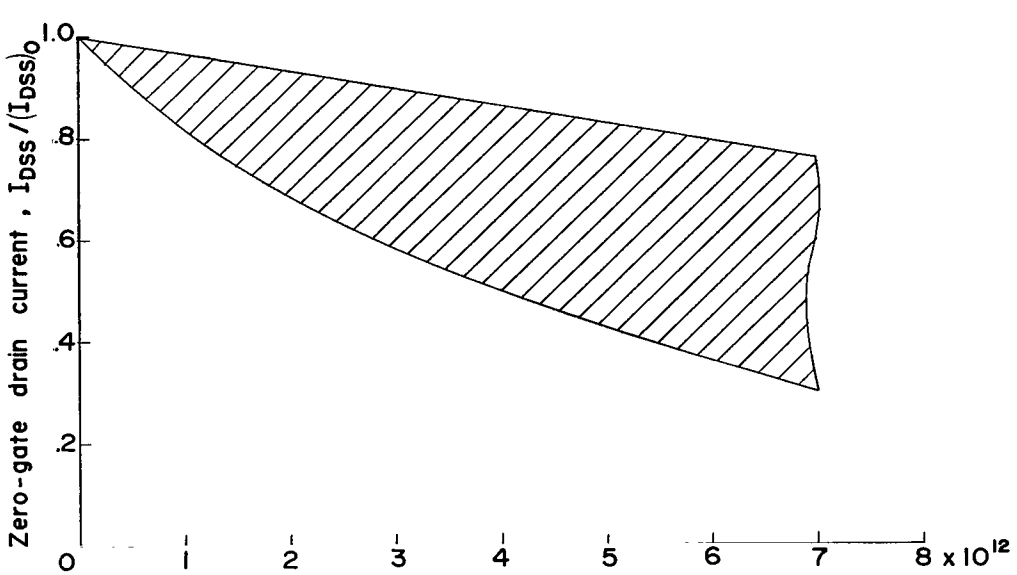

Transistor type D; n-channel Si; epitaxial junction; proton energy = 22 MeV.

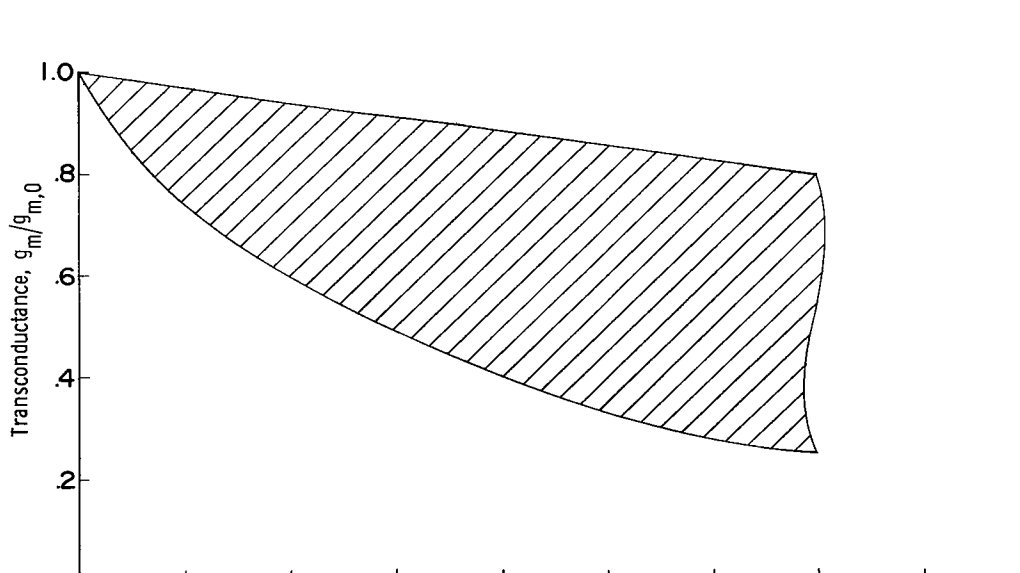

Transistor type D; n-channel Si; epitaxial junction; proton energy = 22 MeV.

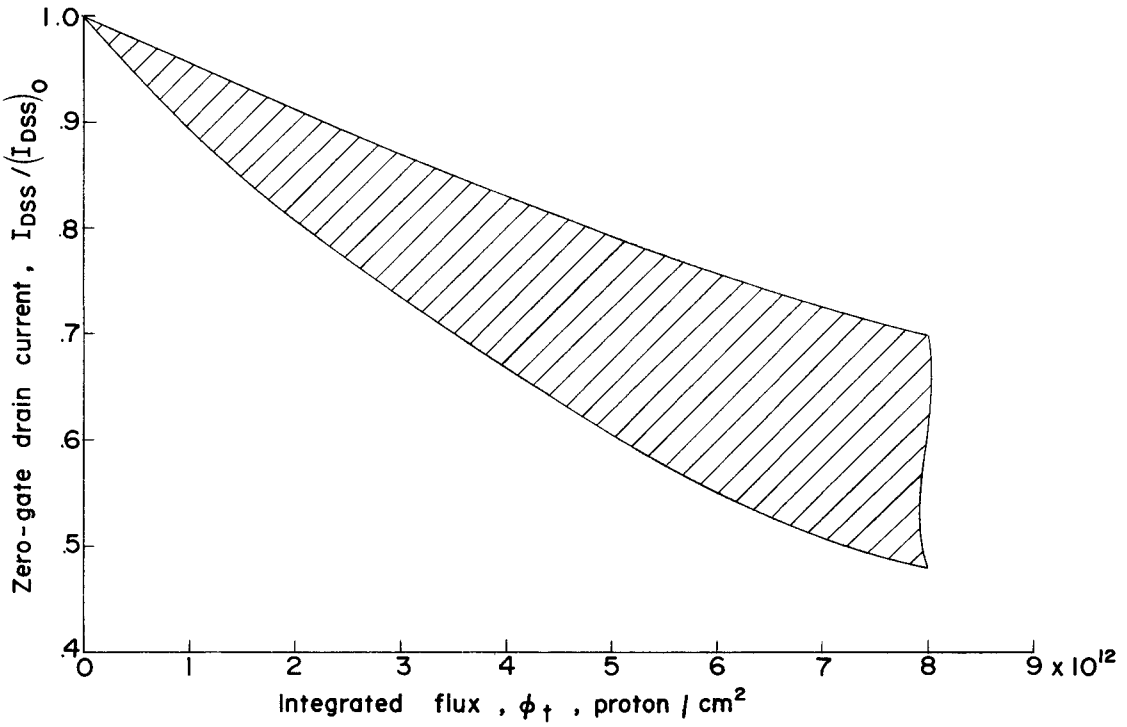

Transistor type E; n-channel Si; planar; proton energy = 22 MeV.

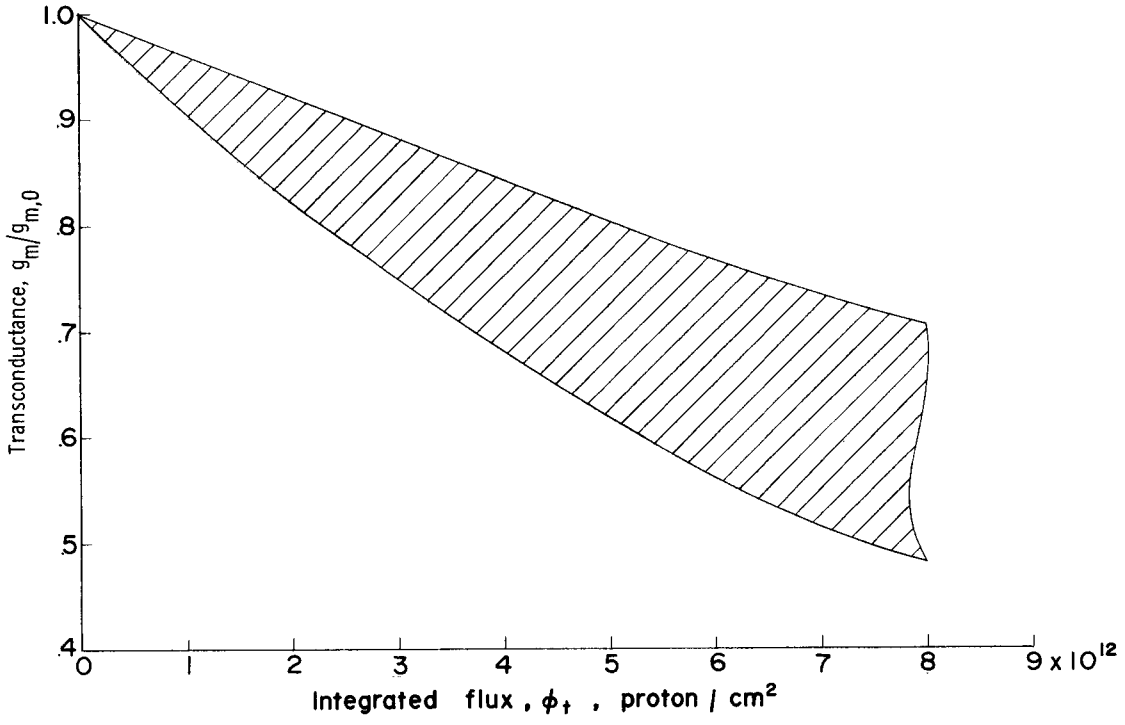

Transistor type E; n-channel Si; planar; proton energy = 22 MeV.

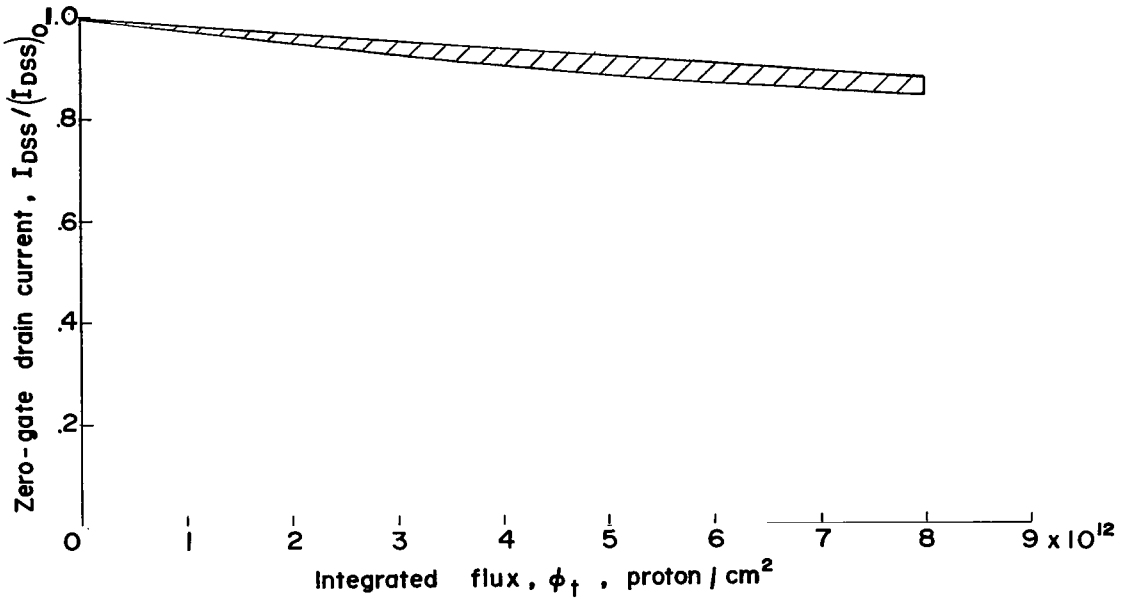

Transistor type F; n-channel Si; epitaxial junction; proton energy = 22 MeV.

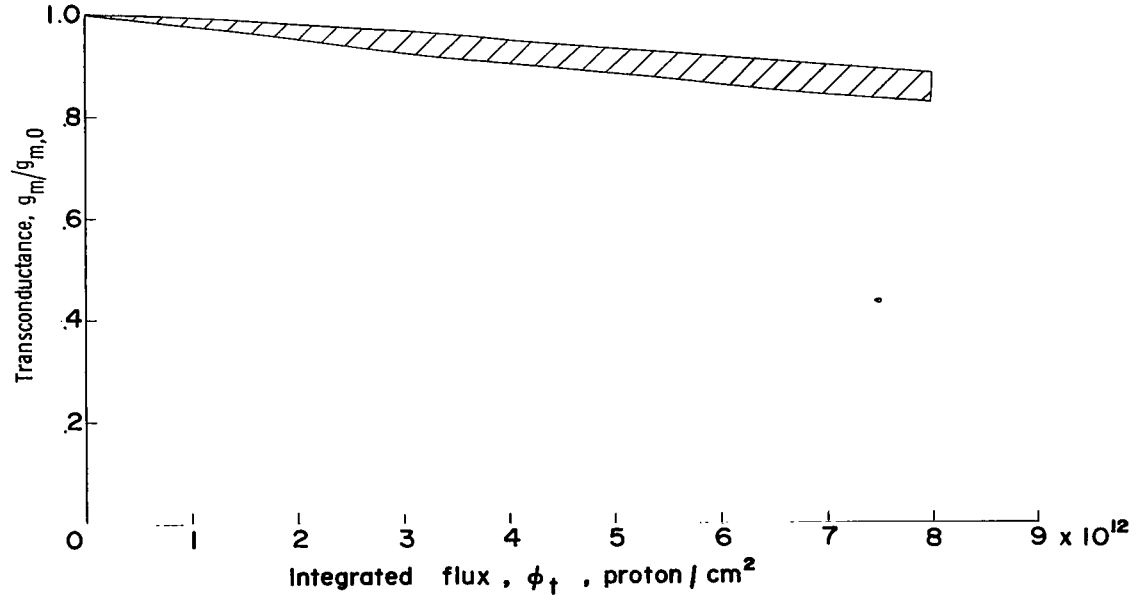

Transistor type F; n-channel Si; epitaxial junction; proton energy = 22 MeV.

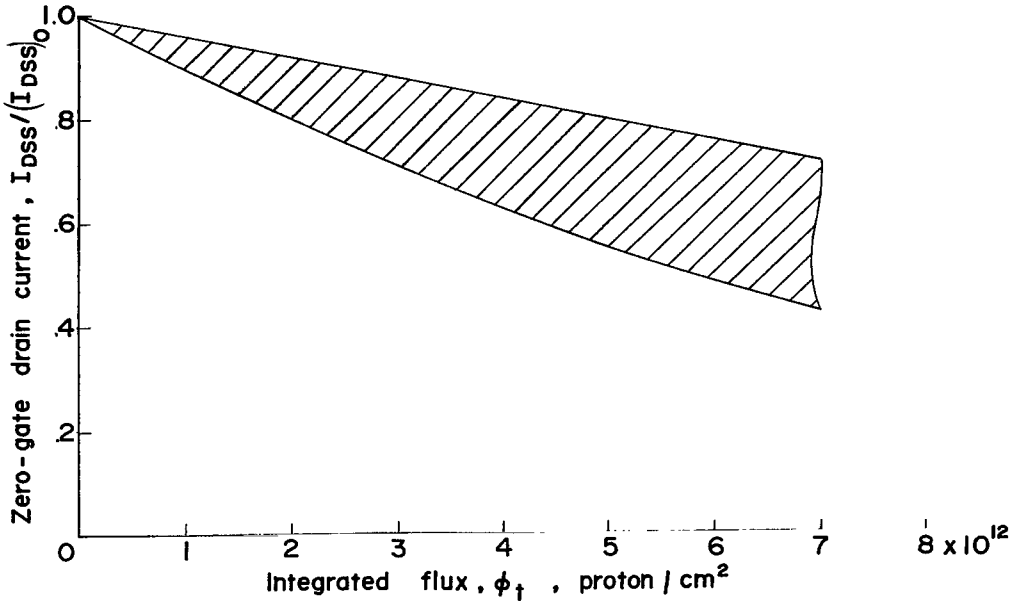

Transistor type G; n-channel Si; epitaxial junction; proton energy = 22 MeV.

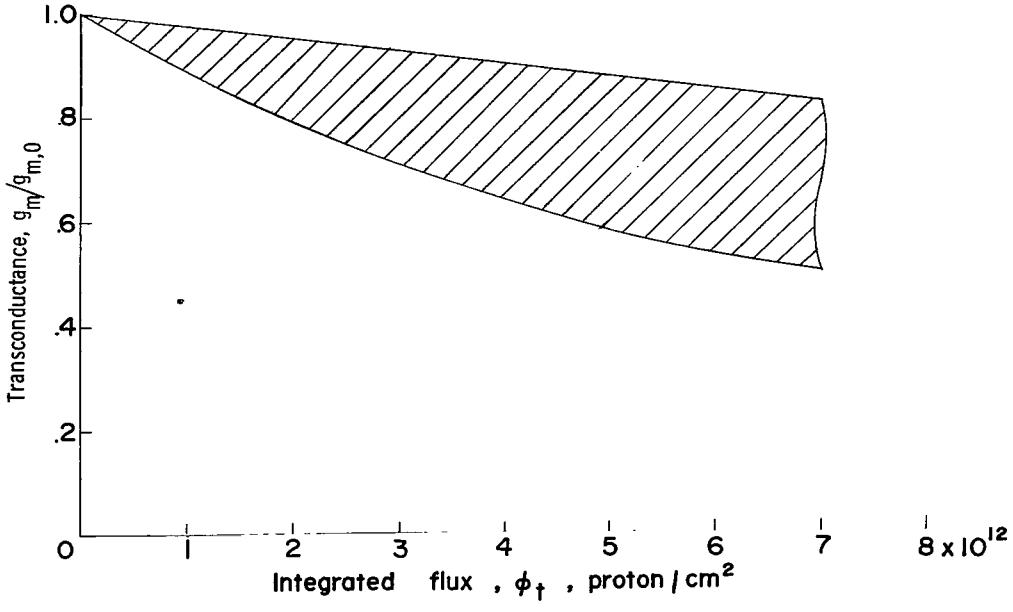

Transistor type G; n-channel Si; epitaxial junction; proton energy = 22 MeV.

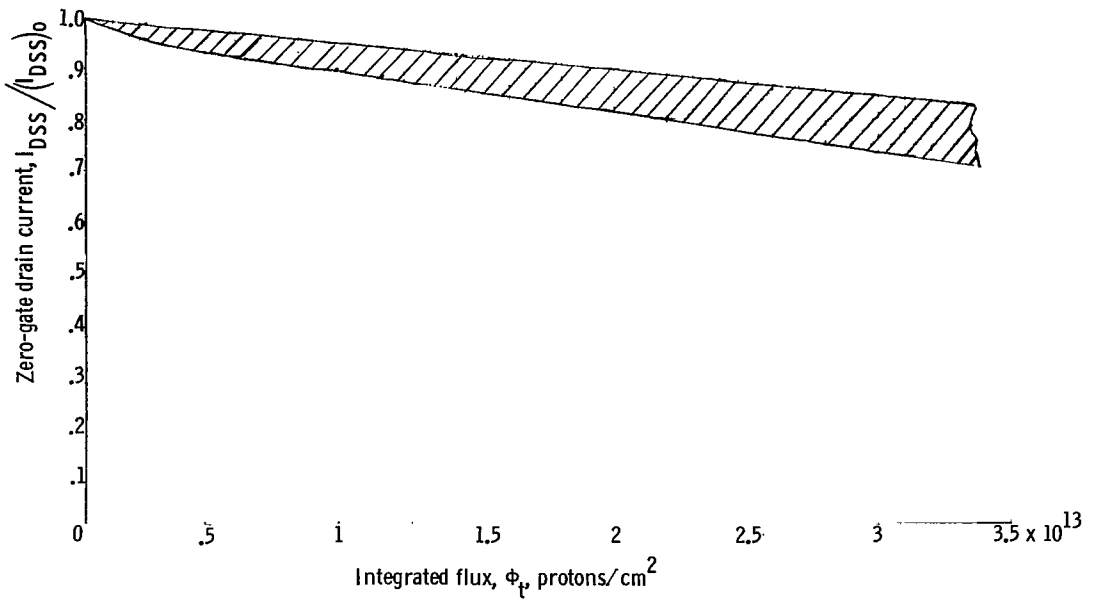

Transistor type H; p-channel Si; planar; proton energy = 128 MeV.

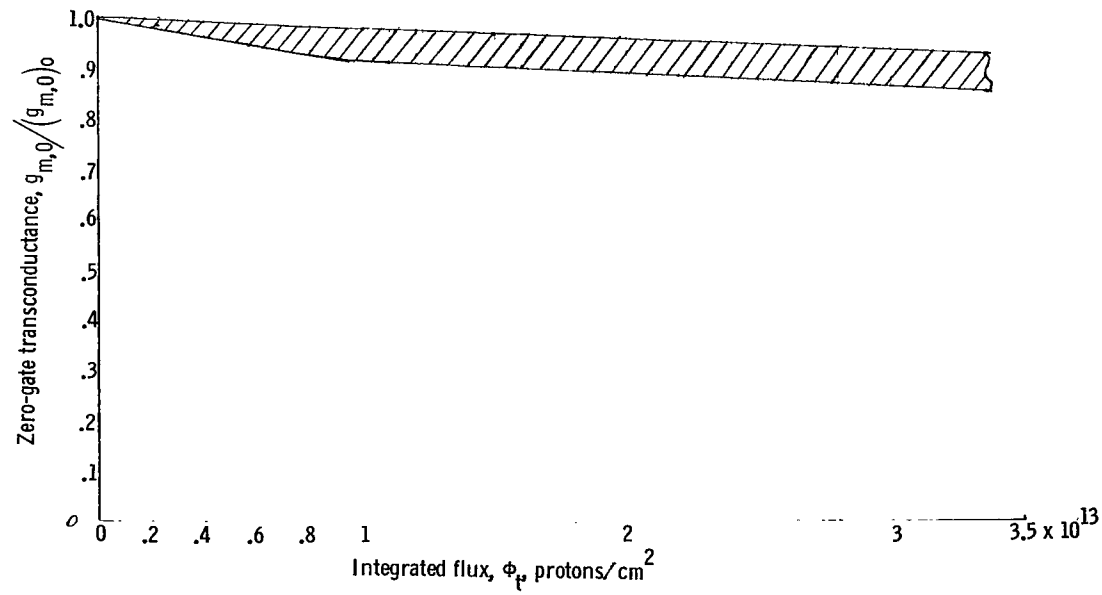

Transistor type H; p-channel Si; planar; proton energy = 128 MeV.

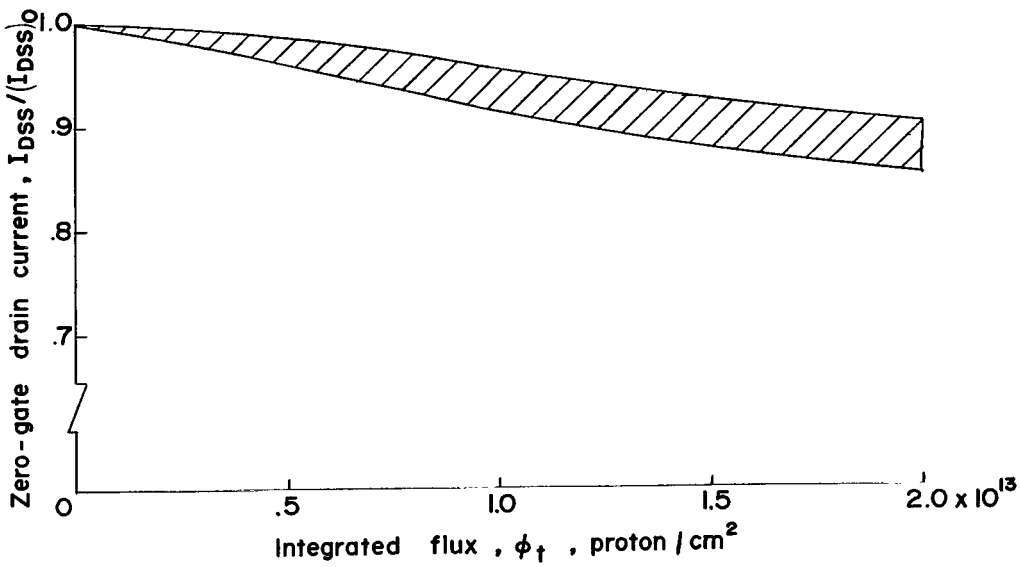

Transistor type K; n-channel Si; epitaxial junction; proton energy = 22 MeV.

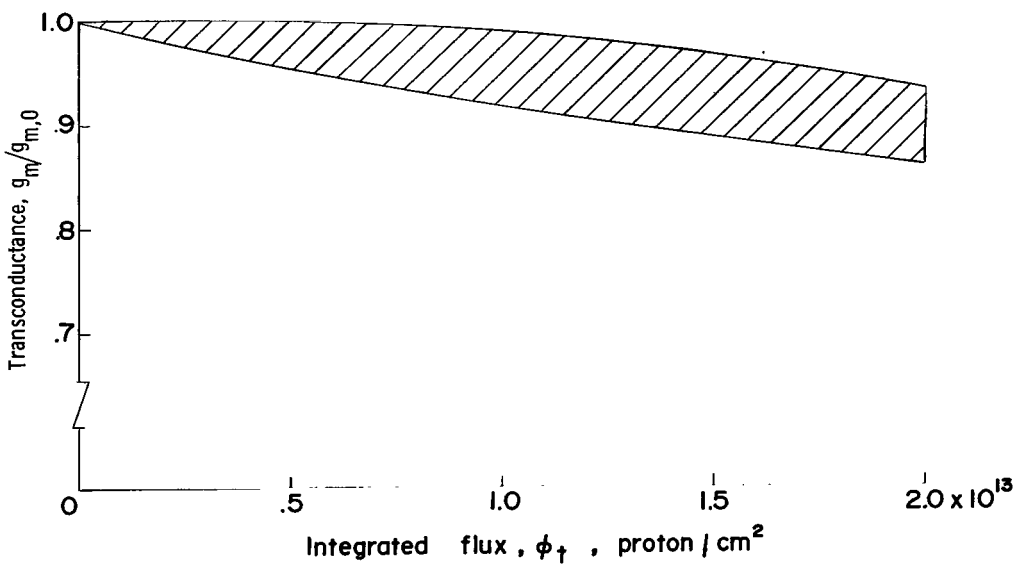

Transistor type K; n-channel Si; epitaxial junction; proton energy = 22 MeV.

REFERENCES

1. Wertheim, G. K.: Energy Levels in Electron-Bombarded Silicon. Phys. Rev., Second ser., vol. 105, no. 6, Mar. 15, 1957, pp. 1730-1735.

2. Breckenridge, Roger A.; and Gross, Chris: Damage to Germanium Due to 22 and 40 MeV Proton Bombardments. NASA TN D-2727, 1965.

3. Van der Ziel, A.: Thermal Noise in Field-Effect Transistors. Proc. IRE, vol. 50, no. 8, Aug. 1962, pp. 1808-1812.

4. Roberts, C. S.; and Hoerni, J. A.: Comparative Effects of 1 Mev Electron Irradiation on Field Effect and Injection Transistors. Field Effect Transistors Tech. Bull. No. 1, Mar. 1963.

5. Kulp. B. A.; Jones, J. P.; and Vetter, A. F.: Electron Radiation Damage in Unipolar Transistor Devices. Proc. IRE (Correspondence), vol. 49, no. 9, Sept. 1961, pp. 1437-1438.

6. Dacey, G. C.; and Ross, I. M.: Unipolar "Field-Effect" Transistor. Proc. IRE, vol. 41, no. 8, Aug. 1953, pp. 970-979.

7. Dacey, G. C.; and Ross, I. M.: The Field-Effect Transistor. Vol. II of Transistor Technology, F. J. Biondi, ed., D. Van Nostrand Co., Inc., c.1958, pp. 517-553.

8. Shockley, W.: A Unipolar "Field-Effect" Transistor. Proc. IRE, vol. 40, no. 11, Nov. 1952, pp. 1365-1376.

9. Richer, I.; and Middlebrook, R. D.: Power-Law Nature of Field-Effect Transistor Experimental Characteristics. Proc. IRE (Correspondence), vol. 51, no. 8, Aug. 1963, pp. 1145-1146.

10. Middlebrook, R. D.: A Simple Derivation of Field-Effect Transistor Characteristics. Proc. IRE (Correspondence), vol. 51, no. 8, Aug. 1963, pp. 1146-1147.

11. Jonscher, A. K.: Principles of Semiconductor Device Operation. John Wiley & Sons, Inc., c.1960.

TABLE I.- PRE-TEST AND POST-TEST DATA ON FIELD-EFFECT TRANSISTORS IRRADIATED AT THE HARVARD UNIVERSITY 168 MeV SYNCHROCYCLOTRON

[First value before irradiation; second value after irradiation]

(a) Transistor type H; p-channel silicon; planar diffused

Transistor	ϕ_t, protons/cm^2	I_{DSS} at V_{DS} = 10V, mA	I_{DGO} at V_{DG} = 10V, μA	I_{SGO} at V_{SG} = 10V, μA	I_{GSS} at V_{GS} = 10V, μA	BV_{DGO} at I_{DGO} = 100 μA, V	V_P at V_{DS} = 10V and I_D = 1 μA, V	g_m at V_{DS} = 10V, V_{GS} = 0, and f = 1 kc, μmhos
7	3.36×10^{13}	1.37 1.05	<0.01 < .01	<0.01 < .01	<0.01 .01	50 88	1.6 1.4	1520 1320
8	3.36×10^{13}	1.30 1.08	<0.01 .05	<0.01 .05	<0.01 .07	62 205	1.3 1.2	1720 1520
9	3.36×10^{13}	1.73 1.48	<0.01 < .01	<0.01 < .01	<0.01 .01	43 53	2.4 2.2	1720 1560
10	3.36×10^{13}	2.05 1.67	<0.01 .02	<0.01 .015	<0.01 .03	45 95	2.4 2.2	1840 1640
11	3.36×10^{13}	1.46 1.21	<0.01 < .01	<0.01 < .01	<0.01 .01	47 57	2.0 1.8	1600 1480

(b) Transistor type J; n-channel germanium; alloy junction

Transistor	ϕ_t, protons/cm^2	I_{DSS} at V_{DS} = 10V, mA	I_{DGO} at V_{DG} = 10V, μA	I_{SGO} at V_{SG} = 10V, μA	I_{GSS} at V_{GS} = 10V, μA	BV_{DGO} at I_{DGO} = 100 μA, V	V_P at V_{DS} = 10V and I_D = 1 μA, V	g_m at V_{DS} = 10V, V_{GS} = 0, and f = 1 kc, μmhos
38	3.36×10^{13}	1.13 .41	1.56 33.00	1.50 29.00	1.50 38.00	63 24	5.6 3.4	510 258
39	6.72×10^{12}	1.07 .79	2.12 9.10	1.92 8.50	2.00 16.00	92 98	3.4 3.4	816 680
40	6.72×10^{12}	1.22 .94	1.62 8.70	1.46 10.00	1.62 10.00	95 108	3.6 3.6	840 730
43	6.72×10^{12}	1.18 .88	1.86 7.70	1.85 9.20	1.90 9.00	85 90	4.6 4.0	690 560
44	6.72×10^{12}	1.25 1.04	1.67 10.00	1.45 8.10	1.80 10.00	82 90	4.2 4.2	830 778

TABLE II.- PRE-TEST AND POST-TEST DATA ON FIELD-EFFECT TRANSISTORS IRRADIATED

AT THE OAK RIDGE NATIONAL LABORATORY 22 MeV CYCLOTRON

[First value before irradiation; second value after irradiation]

(a) Transistor type A; n-channel silicon; epitaxial junction

Transistor	ϕ_t, protons/cm^2	I_{DSS} at V_{DS} = 30V, mA	I_{DGO} at V_{DG} = 30V, nA	I_{SGO} at V_{SG} = 30V, nA	I_{GSS} at V_{GS} = 30V, nA	I_{DGO} at V_{DG} = 100V, nA	g_m at V_{DS} = 30V and f = 5 kc, μmhos	V_P at V_{DS} = 20V and I_D = 0.5 nA, V	y_{is} at V_{DS} = 30V and f = 1 kc, μmhos
40	5×10^{12}	0.54 .37	0.052 2.500	0.10 4.40	0.11 4.20	0.070 3.000	500 380	3.3 3.6	0.100 .136
41	2×10^{12}	0.43 .37	0.036 1.100	0.09 1.60	0.14 1.80	0.044 1.300	460 420	2.6 3.4	0.104 .120
42	2×10^{12}	0.34 .30	0.006 3000	0.030 10 000	0.42 11 000	0.042 3200	430 430	1.85 1.90	0.088 1.240
43	4×10^{12}	0.55 .38	0.040 60.0	0.17 64.00	0.20 50.00	0.084 40.00	480 380	2.45 2.50	0.096 .340
45	4×10^{12}	0.46 .22	0.015 9.000	0.100 12.000	0.11 14.00	[a]330 400	450 260	2.95 (0.5 nA) 3.10 (2 nA)	----
46	5×10^{12}	0.275 .175	0.040 1100.0	0.15 1000.0	0.17 1100.0	[a]85 84	400 280	1.9 (0.5 nA) 1.8 (1 μA)	----

[a] $BV_{DGO}(I_{DGO} = 1\ \mu A)$.

(b) Transistor type B; p-channel silicon; diffused junction

Transistor	ϕ_t, protons/cm^2	I_{DSS} at V_{DS} = -10V, mA	I_{DGO} at V_{DG} = -10V, nA	I_{SGO} at V_{SG} = -10V, nA	I_{GSS} at V_{GS} = 30V and V_{DS} = 0, nA	BV_{DGO} at I_{DG} = 1 μA, V	g_m at V_{DS} = -10V, V_{GS} = 0, and f = 1 kc, μmhos	V_P at V_{DS} = -5V and I_D = 1 μA, V	R_{in} at 2V, ohms
66	7.97×10^{12}	18.5 13.0	1.2 11.5	1.4 13.0	6.0 2.0	44 85	7000 6400	-5.3 -4.4	0.7 6.5
67	9.96×10^{12}	15.5 10.5	1.8 12.0	1.5 13.0	3.2 23.0	49 66	6800 6000	-6.5 -5.3	1.0 6.2
68	6.5×10^{12}	21.0 17.0	0.34 4.0	0.32 4.0	2.5 13.0	44 61	6600 6400	-5.3 -4.6	0.16 1.80
70	6.65×10^{12}	17.5 14.5	1.0 7.5	1.0 7.5	2.9 14.5	41 66	7600 7200	-5.7 -5.2	0.64 3.60
71	6.5×10^{12}	21.0 17.5	0.22 3.60	0.25 3.60	0.98 7.00	40 52	6800 6600	-5.3 -4.6	0.12 1.8

TABLE II.- PRE-TEST AND POST-TEST DATA ON FIELD-EFFECT TRANSISTORS IRRADIATED AT THE OAK RIDGE NATIONAL LABORATORY 22 MeV CYCLOTRON – Continued

(c) Transistor type C; p-channel silicon; planar diffused junction

Transistor	ϕ_t, protons/cm^2	I_{DSS} at V_{DS} = 5V, mA	I_{DGO} at V_{DG} = 30V, nA	I_{SGO} at V_{SG} = 30V, nA	I_{GSS} at V_{GS} = 30V and V_{DS} = 0, nA	BV_{DGO} at I_{DG} = 1 μA and V_{DS} = 0, V	g_m at f = 1 kc and V_{DS} = 5V, μmhos	V_P at V_{DS} = -5V and I_D = -1 μA, V	y_{is} at f = 1 kc and V_{DS} = 5V, μmhos
28	3×10^{12}	0.65 .50	2.90 9.00	1.40 9.00	3.40 13.00	56 51	1800 1500	0.84 .75	0.26 .28
29	2×10^{12}	1.80 1.57	0.98 4.40	1.00 4.40	1.40 7.40	70 120	2900 2800	1.27 1.20	0.26 .26
30	2×10^{12}	1.52 1.31	0.82 6.00	0.76 10.00	1.20 5.00	35 34	2500 2200	1.48 1.40	0.22 .28
31	2×10^{12}	1.65 1.28	0.86 7.00	1.30 7.00	1.60 10.00	60 105	2500 2200	1.45 1.30	0.22 .28
32	2×10^{12}	0.62 .51	1.00 5.00	1.80 6.00	1.90 10.00	73 115	1660 1460	1.05 0.95	0.26 .28
33	8×10^{12}	0.68 .275	1.40 15.0	1.70 16.0	3.20 30.00	98 98	1800 1040	0.81 .61	---
34	5×10^{12}	0.59 .26	2.4 8.8	2.3 9.0	3.0 17.0	62 80	1740 1140	0.71 .51	---
35	4×10^{12}	0.530 .255	4.6 15.0	3.2 15.0	6.4 28.0	58 77	1840 1200	0.66 .50	---

(d) Transistor type D; n-channel silicon; epitaxial junction

Transistor	ϕ_t, protons/cm^2	I_{DSS} at V_{DS} = 10V, mA	I_{DGO} at V_{DG} = 10V, nA	I_{SGO} at V_{SG} = 10V, nA	I_{GSS} at V_{GS} = 30V, nA	BV_{DGO} at I_{DG} = 1 μA and V_{DS} = 0, V	g_m at f = 1 kc, V_{GS} = 0, and V_{DS} = 5V μmhos	V_P at V_{DS} = 15 and I_D = 1 μA, V
7	4×10^{12}	0.78 .133	0.007 10.00	0.010 18.000	0.015 23.000	114 125	680 192	2.15 1.45
8	7×10^{12}	0.98 .34	0.020 7.000	0.072 13.000	0.080 15.000	163 164	680 320	2.8 2.2
9	6×10^{12}	0.91 .53	0.003 4.200	0.034 7.000	0.040 7.800	162 163	680 460	2.6 2.3
10	7×10^{12}	0.68 .37	0.001 4.000	0.006 7.600	0.009 8.000	160 160	6.20 4.00	2.1 1.8

TABLE II.- PRE-TEST AND POST-TEST DATA ON FIELD-EFFECT TRANSISTORS IRRADIATED AT THE OAK RIDGE NATIONAL LABORATORY 22 MeV CYCLOTRON – Continued

(e) Transistor type E; n-channel silicon; planar diffused junction

Transistor	ϕ_t, protons/cm^2	I_{DSS} at V_{DS} = 30V, mA	I_{DGO} at V_{DG} = 30V, pA	I_{SGO} at V_{SG} = 30V, pA	I_{GSS} at V_{GS} = 30V, nA	I_{DGO} at V_{DG} = 100V, nA	g_m at V_{DS} = 30V, f = 5 kc, and V_{GS} = 0, μmhos	V_p at V_{DS} = 20V and I_D = 1 nA, V	y_{is} at V_{DS} = 30V and f = 1 kc, μmhos
53	5.35×10^{12}	1.13 .61	50 6000	80 7200	0.11 8.60	0.08 .90	1120 720	3.60 2.35	0.116 .140
54	3×10^{12}	2.30 1.76	54 200	90 200	0.10 .20	0.18 200.0	1560 1320	3.30 2.95	0.120 1.560
55	2×10^{12}	2.05 2.05	27 3400	13 3200	0.15 3.40	6.0 3.4	1640 1600	3.0 3.0	0.104 6.800
56	2×10^{12}	1.54 1.30	120 3000	78 4400	0.18 5.20	0.3 4.4	1520 1440	2.62 2.10	0.110 .146
59	7.8×10^{12}	1.35 .75	70 9000	150 13 000	0.16 16.00	[a]216 240	1160 680	4.5 5.2 (3 nA)	----
60	1×10^{13}	1.65 .90	38 17 000	60 24 000	82 30 000	[a]221 245	1600 760	2.7 4.9 (7 nA)	----

[a] $BV_{DGO}(I_{DGO} = 1\ \mu A)$.

(f) Transistor type F; n-channel silicon; epitaxial junction

Transistor	ϕ_t, protons/cm^2	I_{DSS} at V_{DS} = 15V, mA	I_{DGO} at V_{DG} = 15V, nA	I_{SGO} at V_{SG} = 15V, nA	I_{GSS} at V_{GS} = 15V, nA	I_{DGO} at V_{DG} = 40V, nA	g_m at f = 1 kc and V_{DS} = 15V, μmhos	V_P at V_{DS} = 15V and I_D = 1 μA, V	y_{is} at V_{DS} = 15V and f = 1 kc, μmhos
23	1×10^{13}	1.25 1.05	0.016 4.80	0.018 6.00	0.024 6.00	0.022 4.60	760 640	5.4 5.3	0.116 .240
24	1×10^{12}	2.21 2.15	0.013 170	0.013 170	0.021 170	0.018 170	920 900	5.0 5.1	0.120 .140
25	4×10^{12}	2.55 2.36	0.006 3.20	0.010 4.00	0.014 4.00	0.022 3.40	920 880	5.0 4.9	0.116 .480

TABLE II.- PRE-TEST AND POST-TEST DATA ON FIELD-EFFECT TRANSISTORS IRRADIATED AT THE OAK RIDGE NATIONAL LABORATORY 22 MeV CYCLOTRON – Continued

(g) Transistor type G; n-channel silicon; epitaxial junction

Transistor	ϕ_t, protons/cm^2	I_{DSS} at V_{DS} = 10V, nA	I_{DGO} at V_{DG} = 10V, nA	I_{SGO} at V_{SG} = 10V, nA	I_{GSS} at V_{GS} = -10V, nA	I_{DGO} at V_{DG} = 15V, nA	g_m at V_{DS} = 10V, V_{GS} = 0, and f = 1 kc, μmhos	V_P at V_{DS} = 15V and I_D = 1 μA, V	y_{is} at V_{DS} = 10V and f = 1 kc, μmhos
18	1×10^{12}	0.52 .49	0.8 2.2	1.2 2.8	1.5 3.6	1.10 4.00	340 320	2.75 2.70	0.10 .132
19	7×10^{12}	0.65 .29	0.025 14.00	0.034 15.00	0.050 12.00	0.034 12.00	360 198	3.50 2.90	0.10 .172
20	4×10^{12}	0.67 .53	0.026 1000	0.030 1000	0.042 1000	0.030 740	380 320	3.20 3.00	0.10 2.70
21	2×10^{12}	0.66 .54	0.14 800	0.14 800	0.16 780	0.17 740	360 320	3.40 3.30	0.10 2.80

(h) Transistor type H; p-channel silicon; planar diffused junction

Transistor	ϕ_t, protons/cm^2	I_{DSS} at V_{DS} = 10V, mA	I_{DGO} at V_{DG} = 10V, μA	I_{SGO} at V_{SG} = 10V, μA	I_{GSS} at V_{GS} = 10V, μA	BV_{DGO} at I_{DG} = 100 μA, V	V_P at V_{DS} = 10V and I_D = 10 μA, V	g_m at V_{DS} = 10V and f = 1 kc, μmhos
46	5.34×10^{13}	1.25 .83	<0.01 .04	<0.01 .04	0.01 .06	60 175	1.4 1.2	1480 1140
47	5.34×10^{13}	1.95 1.17	<0.01 < .01	<0.01 < .01	<0.01 .02	56 170	1.8 1.4	1840 1420
48	5.34×10^{13}	1.30 .60	<0.01 .03	<0.01 .03	<0.01 .04	29 32	1.4 1.0	1760 1144
49	5.34×10^{13}	1.86 .90	<0.01 .06	<0.01 .06	0.01 .09	35 61	1.8 1.2	1800 1260
50	5.34×10^{13}	1.71 .96	<0.01 .01	<0.01 .01	<0.01 .02	59 190	2.0 1.4	1720 1260

TABLE II.- PRE-TEST AND POST-TEST DATA ON FIELD-EFFECT TRANSISTORS IRRADIATED AT THE OAK RIDGE NATIONAL LABORATORY 22 MeV CYCLOTRON – Concluded

(i) Transistor type J; n-channel germanium; alloy junction

Transistor	ϕ_t, protons/cm^2	I_{DSS} at V_{DS} = 10V, mA	I_{DGO} at V_{DG} = 10V, μA	I_{SGO} at V_{SG} = 10V, μA	I_{GSS} at V_{GS} = 10V, μA	BV_{DGO} at I_{DS} = 100 μA, V	V_P at V_{DS} = 10V and I_{DS} = 10 μA, V	g_m at V_{DS} = 10V and f = 1 kc, μmhos
34	5.34×10^{13}	0.65 .56	1.5 .97	1.45 1.20	1.55 1.05	68 67	3.4 3.0	380 360
35	5.34×10^{13}	0.59 .51	2.27 2.15	2.15 2.30	2.35 2.30	81 81	3.2 3.0	550 500
41	5.34×10^{13}	0.94 .84	1.50 1.45	1.55 1.55	1.55 1.48	82 82	3.4 3.0	594 560
42	5.34×10^{13}	1.06 1.06	2.22 1.96	2.25 2.00	2.15 2.00	78 77	4.0 3.8	716 740
45	5.34×10^{13}	1.03 .65	1.75 1.60	1.75 1.90	1.85 1.64	87 85	3.0 2.4	754 540

(j) Transistor type K; n-channel silicon; epitaxial junction

Transistor	ϕ_t, protons/cm^2	I_{DSS} at V_{DS} =15V and V_{GS} = 0, mA	I_{DGO} at V_{DG} = 15V, pA	I_{SGO} at V_{SG} = 15V, pA	BV_{DGO} at I_D = 1 μA, V	V_P at V_{DS} = 10V and I_{DS} = 10, μA	g_m at V_{DS} = 10V, V_{GS} = 0, and f = 0, μmhos
1	2×10^{13}	2.65 2.25	18 2300	36 3400	200 196	5.08 4.93	700 600
2	2×10^{13}	2.50 2.33	44 3000	60 5000	35 35	4.43 4.34	917 850

"The aeronautical and space activities of the United States shall be conducted so as to contribute . . . to the expansion of human knowledge of phenomena in the atmosphere and space. The Administration shall provide for the widest practicable and appropriate dissemination of information concerning its activities and the results thereof."

—NATIONAL AERONAUTICS AND SPACE ACT OF 1958

NASA SCIENTIFIC AND TECHNICAL PUBLICATIONS

TECHNICAL REPORTS: Scientific and technical information considered important, complete, and a lasting contribution to existing knowledge.

TECHNICAL NOTES: Information less broad in scope but nevertheless of importance as a contribution to existing knowledge.

TECHNICAL MEMORANDUMS: Information receiving limited distribution because of preliminary data, security classification, or other reasons.

CONTRACTOR REPORTS: Technical information generated in connection with a NASA contract or grant and released under NASA auspices.

TECHNICAL TRANSLATIONS: Information published in a foreign language considered to merit NASA distribution in English.

TECHNICAL REPRINTS: Information derived from NASA activities and initially published in the form of journal articles.

SPECIAL PUBLICATIONS: Information derived from or of value to NASA activities but not necessarily reporting the results of individual NASA-programmed scientific efforts. Publications include conference proceedings, monographs, data compilations, handbooks, sourcebooks, and special bibliographies.

Details on the availability of these publications may be obtained from:

SCIENTIFIC AND TECHNICAL INFORMATION DIVISION

NATIONAL AERONAUTICS AND SPACE ADMINISTRATION

Washington, D.C. 20546